Medicinal Chemistry Research (2023) 32:2299–2324
https://doi.org/10.1007/s00044-023-03126-7

MEDICINAL CHEMISTRY RESEARCH

ORIGINAL RESEARCH ARTICLE

Structural and stereochemical determinants for hGAT3 inhibition: development of novel conformationally constrained and substituted analogs of (*S*)-isoserine

F. Bavo[1] · S. Kickinger[1] · M. E. K. Lie[1] · C. Avgerinos[1] · Y Xu[1] · K. S. Wilhelmsen[1] · P. Wellendorph[1] · B. Frølund[1]

Received: 12 May 2023 / Accepted: 19 July 2023 / Published online: 16 August 2023

Abstract

The GABA transporter 3 (GAT3) is a member of the GABA transporter (GAT) family proposed to have a role in regulating tonic inhibition. The GAT3-preferring substrate (*S*)-isoserine has shown beneficial effects in a mouse model of stroke accompanied by an increased GAT3 expression, indicating a molecular mechanism mediated by GAT3. However, (*S*)-isoserine is not ideally suited for in vivo studies due to a lack of selectivity and brain permeability. To elucidate the structural determinants of (*S*)-isoserine for GAT3 inhibition, and to optimize and inform further ligand development, we here present the design, synthesis and pharmacological evaluation of a series of conformationally constrained isoserine analogs with defined stereochemistry. Using [^{3}H]GABA uptake assays at recombinant human GAT3, we identified the azetidine and pyrrolidine analogs (2*S*,2´*S*)-**6** and (2*S*,2´*S*)-**7** as the most potent inhibitors. To further elaborate on the selectivity profile both compounds were tested at all GATs, the taurine transporter (TauT) and $GABA_A$ receptors. Although (2*S*,2´*S*)-**6** and (2*S*,2´*S*)-**7** are comparable to (*S*)-isoserine with respect to potency, the selectivity vs. the taurine transporter was significantly improved (at least 6 and 53 times more activity at hGAT3, respectively). A subsequent comprehensive structure-activity study showed that different connectivity approaches, stereochemical variations, simple or larger α- and *N*-substituents, and even minor size enlargement of the heterocyclic ring all abrogated GAT3 inhibition, indicating very strict stereochemical and size requirements. The observed structure activity relationships may guide future ligand optimization and the novel ligands ((2*S*,2´*S*)-**6** and (2*S*,2´*S*)-**7**) can serve as valuable tools to validate the proposed GAT3-mediated effect of (*S*)-isoserine such as in functional recovery after stroke and thus help corroborate the relevance of targeting GAT3 and tonic inhibition in relevant brain pathologies.

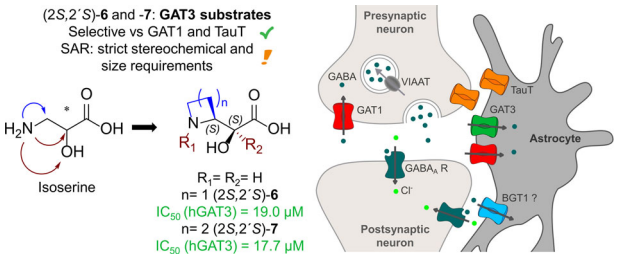

Keywords GAT3 · Isoserine · GABA transporters · Tonic inhibition

Introduction

γ-Aminobutyric acid (GABA) is an important inhibitory neurotransmitter in the mammalian brain. Upon release in high concentration into synapses, GABA reduces the neuronal firing by activating synaptic $GABA_A$ receptors ($GABA_ARs$) in a process called phasic inhibition. Upon

✉ B. Frølund
bfr@sund.ku.dk

[1] Department of Drug Design and Pharmacology, University of Copenhagen, Copenhagen, Denmark

diffusion (spillover), low ambient concentrations of GABA may activate extrasynaptic $GABA_ARs$, reducing the overall neuronal excitability in a process called tonic inhibition [1]. GABAergic inhibition is terminated by GABA transporters (GATs), transmembrane proteins belonging to the solute carrier 6 (SLC6) gene family. Four subtypes of the GATs SLC6 subfamily are responsible for GABA reuptake: GAT1, GAT2, GAT3 and BGT1 (human nomenclature). Among these, the most well-established players in regulating GABA levels in synapses are GAT1 (*SLC6A1*) (expressed in both neurons and astrocytes) [2] and GAT3 (*SLC6A11*) (expressed exclusively in astrocytes). This points to an overall role for GAT1 in regulation of phasic inhibition and GAT3 in regulation of tonic inhibition. The two additional GATs, BGT1 (betaine/GABA transporter, *SLC6A12*) and GAT2 (*SLC6A13*) have a less well-defined role, however, some evidence points to a role for BGT1 in regulation of tonic inhibition [3, 4]. Dysregulated GABAergic signaling is a recurrent hallmark of many neurological and psychiatric diseases [5, 6], also highlighted by recent discoveries of many disease-causing variants, e.g., in GAT1 [7]. Since inhibition of GATs causes an increase of extracellular GABA concentration, GAT blockers have been developed as a therapeutic approach for treating neurological disorders characterized by decreased GABAergic signaling, such as epilepsy [8–11]. So far, the GAT1-selective inhibitor tiagabine is the only FDA (US Food and Drug Administration) approved drug targeting GAT, indicated for the treatment of partial epileptic seizures (Fig. 1) [10]. Recently, in drug discovery, selective inhibition of extrasynaptic GAT3 and BGT1 have been pursued to avoid the numerous side-effects linked to GAT1 inhibition, such as asthenia, dizziness, nervousness, and depression, providing some proof-of-concept for inhibiting extrasynaptic GATs as a way to enhance tonic inhibition [12, 13]. The focus of this study has been GAT3, which is a key target in regulating GABA metabolism via uptake of GABA into astrocytic processes [14] and relevant for both pathologies characterized by increased tonic GABAergic inhibition such as the chronic phase after an ischemic stroke [15] and certain types of absence epilepsy [16]. Thus, pharmacological inhibition of GAT3 represents an interesting strategy for drug development. This has been demonstrated in mouse model of ischemic stroke where chronic treatment with the GAT2/GAT3 preferential substrate (*S*)-isoserine (Fig. 1), has been shown to increase functional recovery in a photothrombotic mouse model of stroke in a dose-dependent manner [17]. Given that (*S*)-isoserine is also a substrate for the taurine transporter (TauT), the goal of this study was to understand the structural determinants of isoserine for GAT3 inhibition, in order to permit future design of more potent and selective GAT3 inhibitors and specifically target GAT3-mediated pathologies.

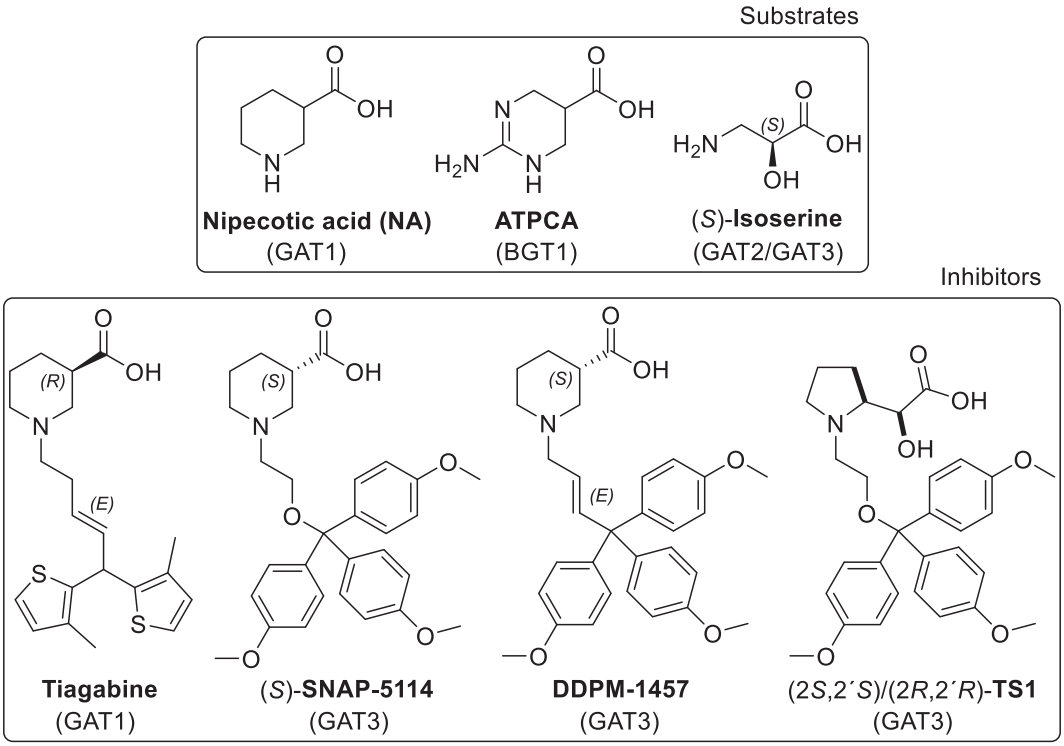

Fig. 1 Chemical structures of reported GAT substrates and inhibitors relevant to this study

Results and discussion

Design strategy

Although efficacious in facilitating post-stroke functional recovery in photothrombotic mouse models [17], (*S*)-isoserine is not an optimal in vivo pharmacological tool. First, although it is selective for extrasynaptic GATs (GAT3, BGT1 and GAT2) over GAT1, it also shows activity at the taurine transporter (TauT), a member of the GATs subgroup responsible for taurine reuptake in both peripheral and brain tissue [17]. Moreover, the high hydrophilicity and the zwitterionic nature of (*S*)-isoserine at physiological pH makes brain permeability unlikely, and discourages systemic administration for CNS related applications [9]. As a result, local chronic administration directly into the infarct via a microosmotic pump was necessary when tested in the photothrombotic stroke mouse model [17]. On the other hand, the simple small structure of (*S*)-isoserine, combined with a proven efficacy in animals, makes it a very attractive starting point for the development of novel optimized extrasynaptic GATs inhibitors.

Since only restricted and scattered information were available on the structural determinants of (*S*)-isoserine for GAT3 inhibition [18], we designed a systematic SAR (structure-activity-relationship) campaign dedicated at elucidating (1) the role of stereochemistry in conformationally constrained alicycles of the flexible (*S*)-isoserine to increase potency and selectivity at the human GAT3 (hGAT3); and (2) the effect of substitution with both conventional and non-conventional lipophilic moieties, in order to increase the likelihood of blood-brain barrier penetration.

Design of locked isoserine analogs: 1–11

Conformational restriction of a flexible ligand into a constrained structure that mimics the bioactive conformation is a common strategy in medicinal chemistry, which often leads to enhanced affinity, potency or selectivity by reducing the entropic penalty upon a binding event [19–22]. Although inhibition of a transporter by a competitive substrate such as (*S*)-isoserine is a more complex process than a specific binding event, several examples of conformationally constrained inhibitors of SLC6 transporters have already been reported [23–25]. Based on this idea, we designed four series of locked isoserine analogs and related variations, with defined stereochemistry in most cases (Fig. 2A). Series 1: the nitrogen was bridged to the α-hydroxy group ((*S*)- and (*R*)-**1**), and the resulting ether oxygen was further replaced with either an amino ((*rac*)-**2**) or a methylene group ((*rac*)-nipecotic acid). Series 2: the amino group was connected to the α-carbon via a 1–3 carbon chain (**3**–**5**). Series 3: the nitrogen was connected to the β-carbon via a 2–4 carbon chain (**6**–**8**). Series 4: the nitrogen of each compound of series 3 was repositioned from the β- to the γ- position, increasing structural similarity to the endogenous ligand GABA (**9**–**11**).

Design of substituted (2*S*,2′*S*)-6 and (2*S*,2′*S*)-7 analogs: 6a–g, 7a–c, g, and 12

As described in detail in the Pharmacology section below, preliminary screening of inhibitory activity of compounds **1**–**11** in a [^{3}H]GABA uptake assay at hGAT3 transiently expressed in tsA201 cells identified compounds (2*S*,2′*S*)-**6** and (2*S*,2′*S*)-**7** as the most promising hGAT3 inhibitors of the four series. The two compounds were therefore selected to investigate the impact of substitution at the α- and *N*-position, both of which are synthetically accessible and privileged in development of GATs inhibitors. To this end, three additional series of compounds were developed (Fig. 2B). Series 5: *N*-substitution is a common approach for development of GATs inhibitors, as exemplified by tiagabine and SNAP-5114 [9, 26] (Fig. 1). Since we previously reported a series of *N*-substituted analogs of 2-amino-1,4,5,6-tetrahydropyrimidine-5-carboxylic acid (ATPCA) as hBGT1 inhibitors where bulky but simple substituents such as phenyl or biphenyl were tolerated [27], a variety of simple substituents were introduced providing (2*S*,2′*S*)-**6a**–**f** and (2 *S*,2′*S*)-**7a**–**c**. Series 6: introduction of a methyl group neighboring a stereocenter of a strained structure is an effective strategy to explore pocket space availability without excessively altering the most favored conformation of a ligand [28]. Therefore, the α-methyl analogs of (2*S*,2′*S*)-**6**, namely (2*S**,2′*S*)-**12** and (2*R**,2′*S*)-**12**, were designed and developed. Series 7: inspired by Steffan et al. [29], who introduced the 2-[tris(4-methoxyphenyl)methoxy]ethyl substituent of (*S*)-SNAP-5114 (IC_{50} value of 1.9 µM at mouse GAT4 (mGAT4), the paralogue of hGAT3) at the nitrogen of the racemic mixture (2*S*,2′*S*)/(2*R*,2′*R*)-**7a** resulting in (2*S*,2′*S*)/(2*R*,2′*R*)-**TS1** (5.8 µM at mGAT4), and by Pabel et al., who developed DDPM-1457, a more chemically stable mGAT4 inhibitor (IC_{50} of 1.3 µM) than (*S*)-SNAP-5114 [30], we decided to *N*-substitute the most potent GAT3 inhibitors (2*S*,2′*S*)-**6** and (2*S*,2′*S*)-**7** with the substituent of DDPM-1457 ((*E*)-4,4,4-tris(4-methoxyphenyl)but-2-en-1-yl), providing (2*S*,2′*S*)-**6g** and (2*S*,2′*S*)-**7g**. Ultimately, due to the unexpected inactivity of (2*S*,2′*S*)-**6g** and (2*S*,2′*S*)-**7g** (see below), we decided to explore which stereochemical determinants were required for hGAT3 activity when the *N*-bulky lipophilic moiety was introduced. We therefore synthesized the three remaining stereoisomers of (2*S*,2′*S*)-**7g**, namely (2*R*,2′*R*)-**7g**, (2*R*,2′*S*)-**7g** and (2*S*,2′*R*)-**7g**.

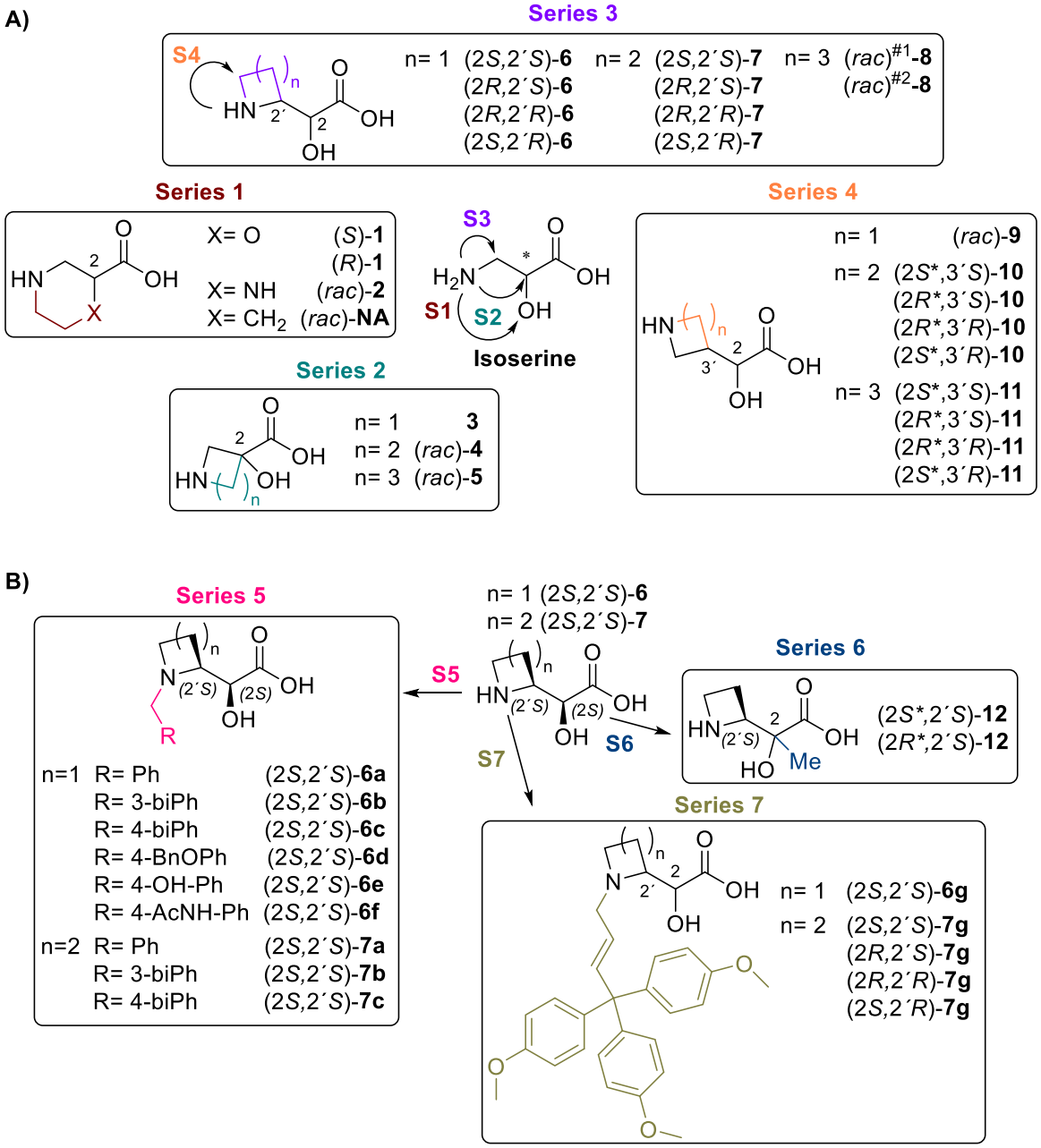

Fig. 2 Structures of the target compounds and their design: **A** locked isoserine analogs, **NA** nipecotic acid; **B** substituted analogs of (2*S*,2´*S*)-**6** and (2*S*,2´*S*)-**7**. When the stereochemistry at one stereocenter remains unknown, an asterisk (*) is added to indicate that the assignment could be the opposite. For the sake of clarity, the two isolated racemic mixtures of **8** with unkonw stereochemistry (2*S**,2´*S**)/(2*R**,2´*R**)-**8** and (2*R**,2´*S**)/(2*S**,2´*R**)-**8** have been aribitrarily identified as (*rac*)$^{\#1}$-**8** and (*rac*)$^{\#2}$-**8**, respectively

Chemistry

The HCl salts of compounds (*S*)-**1** and (*R*)-**1**, (*rac*)-**2** and (*rac*)-nipecotic acid were commercially available and purchased. The HBr salt of compound (*rac*)-**5** was obtained from an in-house library of previously published compounds [31]. Intermediates **13**, **14**, (*S*)- and (*R*)-**17**, (*S*)- and (*R*)-**19**, (*rac*)-**20**, (*S*)- and (*R*)-**24**, (*S*)- and (*R*)-**25**, **26** and **32** were purchased.

Synthesis of rigidified analogs of (*S*)-isoserine: 3, (*rac*)-4 and 6–11

Final compounds **3**, (*rac*)-**4**, and different stereoisomers of **6**–**11** were prepared according to Scheme 1 from commercially available achiral building blocks (for the compounds **3**, (*rac*)-**4** and (*rac*)-**9**), enantiopure starting materials (for all stereoisomers of **6**, **7**, **10** and **11**), or racemic mixture (for the racemic mixture of the diastereoisomers of **8**). (*S*)- or (*R*)-*N*-

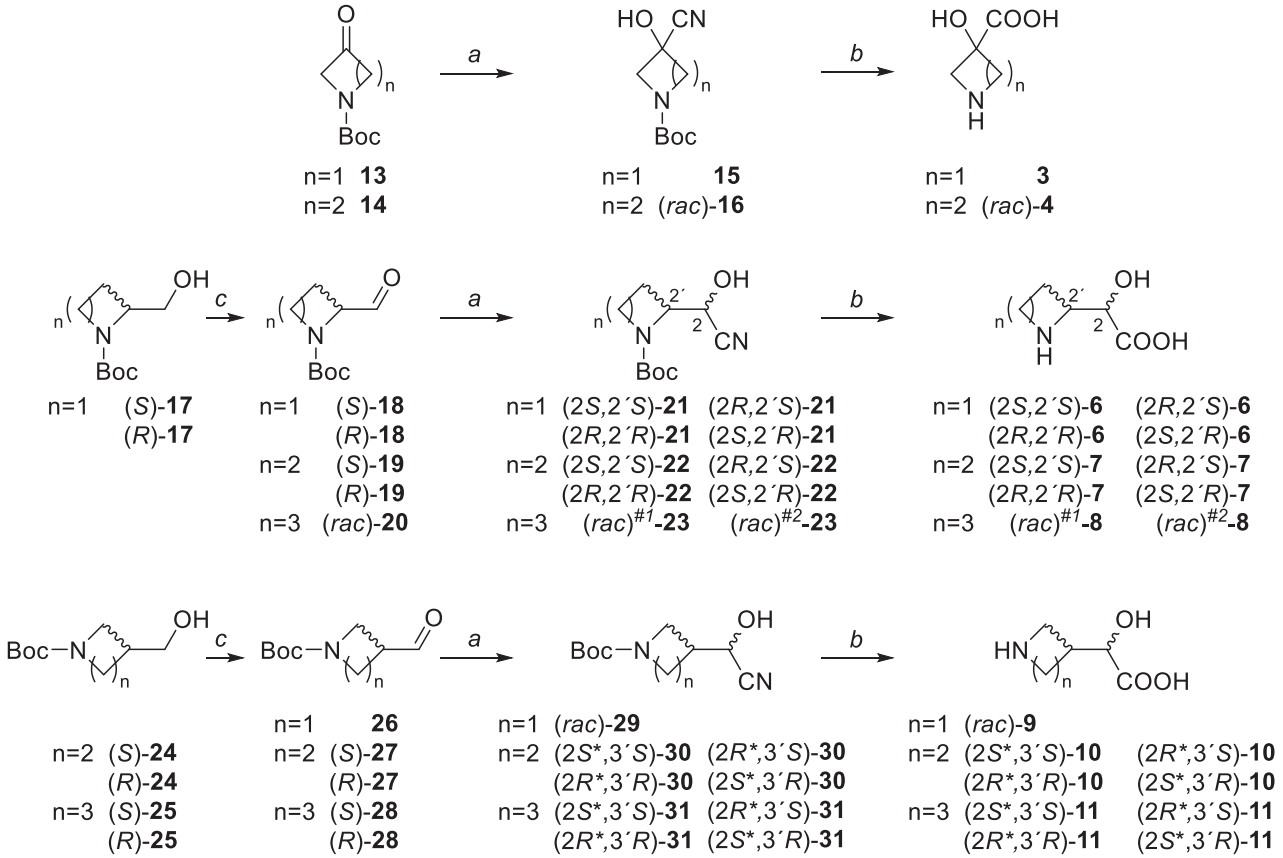

Scheme 1 Reagents and conditions. a $NaHSO_3$, KCN, diethylether/water 1:2, rt, overnight. b HCl 4 M, 85 °C, overnight. c Trichloroisocyanuric acid, TEMPO, DCM, 0 °C to rt, 15 min

Boc-2-hydroxymethyl-azetidine ((*S*)- and (*R*)-**17**), (*S*)- or (*R*)-*N*-Boc-3-hydroxymethyl-pyrrolidine ((*S*)- and (*R*)-**24**) and (*S*)- or (*R*)-*N*-Boc-3-hydroxymethyl-piperidine ((*S*)- and (*R*)-**25**) were oxidized to the corresponding aldehydes (*S*)- or (*R*)-**18**, (*S*)- or (*R*)-**27**, (*S*)- or (*R*)-**28** using 2,2,6,6-tetramethyl-1-piperidinyloxy (TEMPO) and trichloroisocyanuric acid, according to a method that does not induce significant racemization of chiral center at the α-carbon [32]. Together with the commercially available *N*-Boc-3-oxoazetidine (**13**), *N*-Boc-3-oxopyrrolidine (**14**), (*S*)- or (*R*)-*N*-Boc-pyrrolidine-2-carboxyaldehyde ((*S*)- and (*R*)-**19**), (*rac*)-*N*-Boc-piperidine-2-carboxyaldehyde ((*rac*)-**20**) and *N*-Boc-3-formyl-azetidine (**26**), they were converted to the corresponding α-hydroxynitrile analogs by treatment with potassium cyanide (**15**, **16**, **21**, **22**, **23**, **29**, **30**, **31** from **13**, **14**, **18**, **19**, **20**, **26**, **27**, **28** respectively). Whereas the cyanation introduced a second stereocenter (at locant 2) in an asymmetric and enantiopure (or racemic) aldehyde, a pair of diastereoisomers (or diasteromeric pairs of racemic mixtures) was formed.

Diasteroisomers (or diasteromeric pairs of racemic mixtures) were isolated by silica gel flash column chromatography and are listed according to their elution order. As detailed below, the absolute configuration at both locants was determined for (2*S*,2´*S*)- and (2*R*,2´*S*)-**21**, (2*R*,2´*R*)- and (2*S*,2´*R*)-**21**; (2*S*,2´*S*)- and (2*R*,2´*S*)-**22**, (2*R*,2´*R*)- and (2*S*,2´*R*)-**22**. For compounds where the stereochemistry at one of the stereocenters remained unknown, an asterisk (*) was used to indicate that the assignment of that locant could be the opposite: the racemic mixtures (2*S**,2´*S**)/(2*R**,2´*R**)-**23** and (2*R**,2´*S**)/(2*S**,2´*R**)-**23** (for simplicity identify as (*rac*)$^{\#1}$-**23** and (*rac*)$^{\#2}$-**23**, respectively); the steroisomers (2*S**,3´*S*)- and (2*R**,3´*S*)-**30**, (2*R**,3´*R*)- and (2*S**,3´*R*)-**30**; and (2*S**,3´*S*)- and (2*R**,3´*S*)-**31**, (2*R**,3´*R*)- and (2*S**,3´*R*)-**31**.

Acidic hydrolysis of each α-hydroxynitriles **15**, **16**, **21**, **22**, **23**, **29**, **30**, **31** provided respectively the final compounds **3**, the racemic mixture of compounds **4**, each of the four stereoisomers of **6, 7**, the diastereoisomers **8** as racemic mixtures, the racemic mixture **9**, and each of the four stereoisomers of **10** and **11**.

Determination of the absolute configuration of (2*S*,2´*S*)-6 and (2*S*,2´*S*)-7

As described in the Pharmacology section, (2S,2´*S*)-**6** and (2S,2´*S*)-**7** were identified as the two most active and GAT3-selective compounds. Therefore, the absolute

stereochemistry at their newly formed asymmetric carbon (locant 2) was investigated by (1) Mosher analysis (Supplementary Information) of their precursors (2*S*,2´*S*)-**21** and (2*S*,2´*S*)-**22**, B) ^{1}H NMR analysis of (2*S*,2´*S*)- and (2*R*,2´*S*)-**21** combined with conformational analysis (Supplementary Information), and C) comparison with NMR data reported for (2*S*,2´*S*)-**7**. A) According to an established literature protocol, (2*S*,2´*S*)-**21** and (2*S*,2´*S*)-**22** were treated with both (*S*)-(+)- and (*R*)-(−)-α-methoxy-α-(trifluoromethyl)phenylacetyl chloride (MTPA-Cl), providing respectively the (*R*)- and (*S*)-MTPA esters of (2*S*,2´*S*)-**21** and (2*S*,2´*S*)-**22** [33]. Briefly, a Mosher ester adopts a specific conformation in solution, which positions the aromatic ring of the MTPA in front of one of the substituents of the secondary alcohol, thereby exerting an anisotropic, magnetic shielding effect on its protons. ^{1}H NMR analysis showed that the chemical shifts of the azetidinyl and the pyrrolidinyl rings of the (*R*)-MTPA esters were more downfield compared to their corresponding (*S*)-MTPA esters, resulting in a negative $\Delta\delta^{SR}$ and therefore suggesting the configuration at the secondary alcohols (locant 2) to be "*S*": (2*S*,2´*S*)-**21** and (2*S*,2´*S*)-**22**. (2) According to literature, *J* coupling constant analysis of conformationally constrained structures combined with conformational analysis has been used to uneqivocally identify relative configurations of stereocenters [34–36]. As the absolute configuration of the azetidine or pyrrolidine ring (locant 2´) is known, it is possible to deduce the absolute configuration of the newly formed stereocenter. Similarly, aided by relevant 1D- and 2D-NMR recorded in $CDCl_3$, all the ^{1}H signals of the first eluting diasteromer (2*S*,2´*S*)-**21** were assigned, where the signal of the Hα appeared as a doublet coupling only with the mobile proton of the secondary alcohol, but not with the Hβ. According to the Karplus equation, a negligible ^{3}J coupling constant can only occur when the dihedral torsional angle is close to 90°, and it is certainly not possible with in an anti disposition of Hα and Hβ. Contrariwise, the Hα of the second eluting diasteromer (2*R*,2´*S*)-**21** appears as a doublet with a 8.3 Hz coupling constant to Hβ, typical of an anti periplanar disposition between Hα and Hβ. Computational conformational search was carried out in chloroform, to match at best the NMR conditions. The most favorable conformation of both (2*S*,2´*S*)-**21** and (2*R*,2´*S*)-**21** showed an intramolecular H-bond between the OH and the Boc carbonyl, that fixed the Hα at a rather specific torsional angle compared to Hβ: gauche for (2*S*,2´*S*)-**21**, and anti periplanar for (2*R*,2´*S*)-**21**, suggesting the first eluting diasteromer to be (2*S*,2´*S*)-**21** and the second eluting diasteromer to be (2*R*,2´*S*)-**21**. Moreover, the only conformation in which (2*S*,2´*S*)-**21** could reach an anti Hα to Hβ disposition would require the nitrile group to be directed toward the hindered *N*-Boc group and sterically interfere with it. (3) Since (2*S*,2´*S*)-**7** had previously been reported and characterized by NMR in MeOD as a TFA salt, (2*S*,2´*S*)-**7** was converted in the corresponding TFA salt [37]. The NMR spectra were recorded in MeOD and proved to be coherent with those reported in literature, eventually confirming (2*S*,2´*S*)-**7** to have (*S,S*) configuration. Overall, both active compounds (2*S*,2´*S*)-**6** and (2*S*,2´*S*)-**7** (and their precursors (2*S*,2´*S*)-**21** and (2*S*,2´*S*)-**22**) were discovered to have (*S,S*) configuration. Based on NMR identity, (2*R*,2´*R*)-**6** and (2*R*,2´*R*)-**7** (and their precursors) were assigned as the enantiomers with (*R,R*) configuration. Based on NMR diversity, (2*R*,2´*S*)-**6** and (2*R*,2´*S*)-**7** (and precursors) were assigned as the diasteroisomers with (*R,S*) configuration, while (2*S*,2´*R*)-**6** and (2*S*,2´*R*)-**7** (and precursors) as the diastereoisomers with (*S,R*) configuration. To exclude the possibility of racemization in each of the steps of the synthesis, chiral analytical HPLC of final compounds (2*S*,2´*S*)-**6** and (2*S*,2´*S*)-**7** was performed and compared with that of a mechanical mixture of (2*S*,2´*S*)-**6**/(2*R*,2´*R*)-**6** and of (2*S*,2´*S*)-**7**/(2*R*,2´*R*)-**7**, and both proved to have ee >99%.

Synthesis of *N*- or α-substituted compounds (2*S*,2´*S*)-6a–g, (2*S*,2´*S*)-7a–c, 12 and 7g

Compounds (2*S*,2´*S*)-**6a–f** and (2*S*,2´*S*)-**7a–c** were prepared as described in Scheme 2. Briefly, (2*S*,2´*S*)-**6** and (2*S*,2´*S*)-**7** were converted by reductive amination with a variety of aromatic aldehydes providing (2*S*,2´*S*)-**6a–f** and (2*S*,2´*S*)-**6a–c**. The commercially available (*S*)-*N*-Boc-azetidine-2-carboxylic acid (*S*)-**32** was converted into the corresponding Weinreb amide (*S*)-**33**, further treated with methylmagnesiumchloride to afford the ketone (*S*)-**34**, that upon cyanation provided the mixture of enantiopure diasteroisomers (2*S**,2´*S*)- and (2*R**,2´*S*)-**35**, separated by silica gel flash column chromatography and eventually converted into the final compounds (2*S**,2´*S*)-**12** and (2*R**,2´*S*)-**12** by acidic hydrolysis.

Compounds **6g** and **7g** were synthesized according to Scheme 3. Preparation of the methyl esters (2*S*,2´*S*)-**36**, (2*S*,2´*S*)-**37**, (2*R*,2´*S*)-**37**, (2*R*,2´*R*)-**37** and (2*S*,2´*R*)-**37**, followed by alkylation with (*E*)-4,4',4''-(4-bromobut-2-ene-1,1,1-triyl)tris(methoxybenzene) **40**, prepared according to literature [38], provided (2*S*,2´*S*)-**38g** and all the four diasteromers of **39g**, which were finally hydrolyzed in basic conditions to the final compounds (2*S*,2´*S*)-**6g**, (2*S*,2´*S*)-**7g**, (2*R*,2´*S*)-**7g**, (2*R*,2´*R*)-**7g** and (2*S*,2´*R*)-**7g**.

Pharmacology

Stereochemical requirements for hGAT3 inhibition: screening of 1–11 at hGAT3

In order to identify one or more privileged conformationally constrained scaffolds, compounds **1**–**11** and

(*rac*)-nipecotic acid (**NA**) were screened at three different concentrations (10, 100 and 1000 µM) in a [^{3}H]GABA uptake inhibition assay in tsA201 cells transiently expressing hGAT3 (Fig. 3A).

Among the 25 synthesized compounds, three compounds, (2*S*,2´*S*)-**6**, (2*S*,2´*S*)-**7** and (2*S**,3´*S*)-**10** (Fig. 3), showed more than 75% inhibition at hGAT3 (less than 25% residual activity) when tested at 100 µM. For these compounds, full concentration-response curves were obtained and the IC_{50} values determined (IC_{50} values of 19.0, 17.7 and 41.9 µM respectively, Table 1 and Fig. 3).

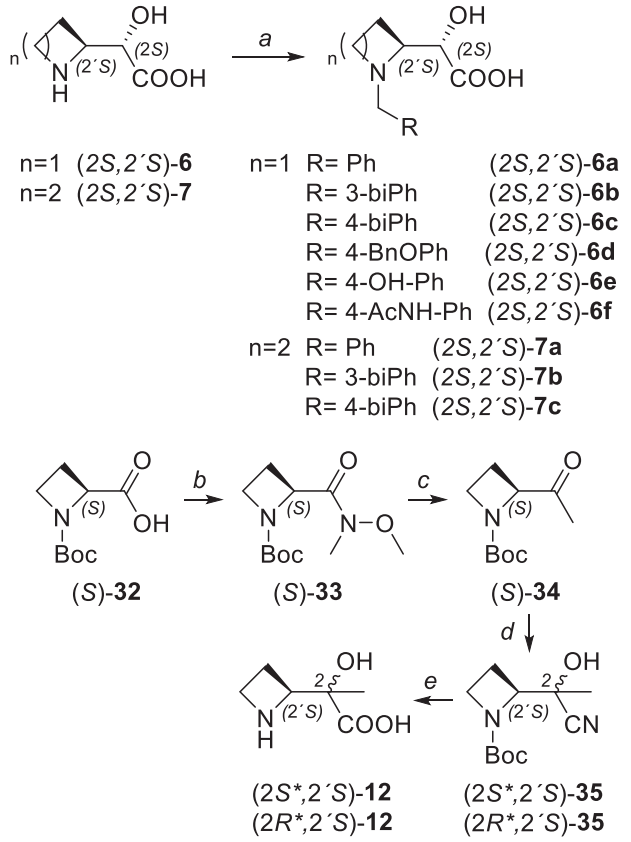

Scheme 2 Reagents and conditions. a $NaBH_3CN$, aldehyde, methanol, 60 °C, overnight. b N,O-dimethylhydroxylamine HCl, DMF, N-Memorpholine, HOBt, EDC, rt, overnight. c dry THF, MeMgCl 3 M in THF, −78 °C, 2 h. d $NaHSO_3$, KCN, diethylether/water 1:2, rt, overnight. e HCl 4 M, 85 °C, overnight

Although reduced conformational flexibility of (*S*)-isoserine did not result in more potent hGAT3 inhibitors, this SAR investigation provided important understanding of structural and stereochemical requirements for hGAT3 inhibition. First, previous literature showed only 3–5 times difference in IC_{50} values between isoserine and its non-hydroxylated analog β-alanine at hGAT3 (7 µM vs. 36 µM), and at mGAT4 (6 µM vs. 22 µM), suggesting that the OH group of isoserine is beneficial, but not required for hGAT3 inhibition [17, 39, 40]. Therefore, the total loss of activity observed when the oxygen of isoserine is incorporated within the morpholine ring of (*S*)- or (*R*)-**1** cannot be exclusively attributed to the absence of an H-bond donor. It is more plausibly related to suboptimal distances and angles between the carboxylic group and the amine, which are key features of GAT inhibitors [41]. This hypothesis was substantiated by both the inactivity of the piperazine analog (*rac*)-**2**, in which the ethereal oxygen (hydrogen bond acceptor) is replaced by an amine (hydrogen bond donor), and by the high-micromolar inhibition of nipecotic acid. Similarly, all of the compounds **3**–**5** in which the terminal amine is connected to the α-carbon were inactive. Consistently with our results, while this manuscript was in preparation, Andreß et al. reported a series of α- and β-hydroxy substituted amino acid derivatives and their inhibition at mGAT4 (which corresponds to hGAT3), where **3** and (*rac*)-**5** were also inactive [18]. In contrast, when we introduced conformational constrain by incorporation of both the β carbon and the nitrogen within heterocyclic amines (**6**–**8**), hGAT3 inhibition was maintained at specific ring size and stereochemical requirements. Azetidine- or pyrrolidine-containing compounds (2*S*,2´*S*)-**6** and (2*S*,2´*S*)-**7** showed similar inhibition at hGAT3 (23 and 21 µM respectively), while the piperidine-based higher homologs **8** were inactive, suggesting limited space surrounding the alicycle at the orthosteric binding site of hGAT3. In both cases, only the *S*,*S* stereoisomers were active. (2*S*,2´*S*)-**7** is therefore the pharmacologically active eutomer of the

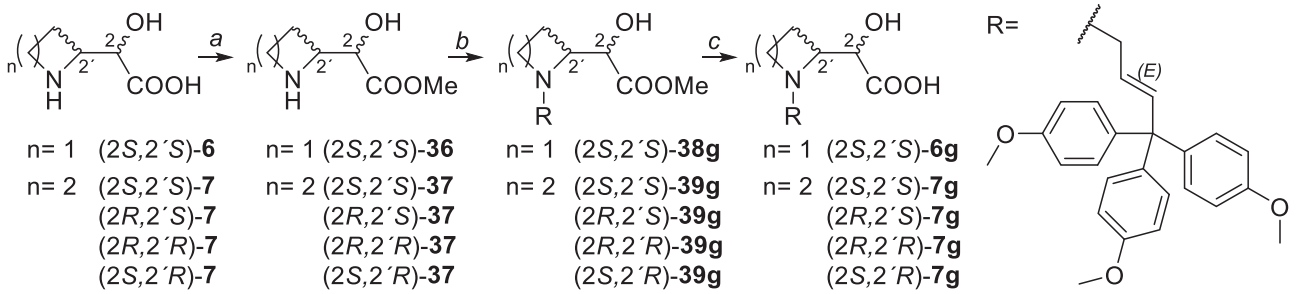

Scheme 3 Reagents and conditions. a $SOCl_2$, methanol, rt, overnight. b K_2CO_3, KI, (E)-4,4',4"-(4-bromobut-2-ene-1,1,1-triyl)tris(methoxybenzene) **40**, acetone/DMF/ACN 1:1:1, rt, overnight, dark. c LiOH 2 M, water/dioxane, rt, 2 h

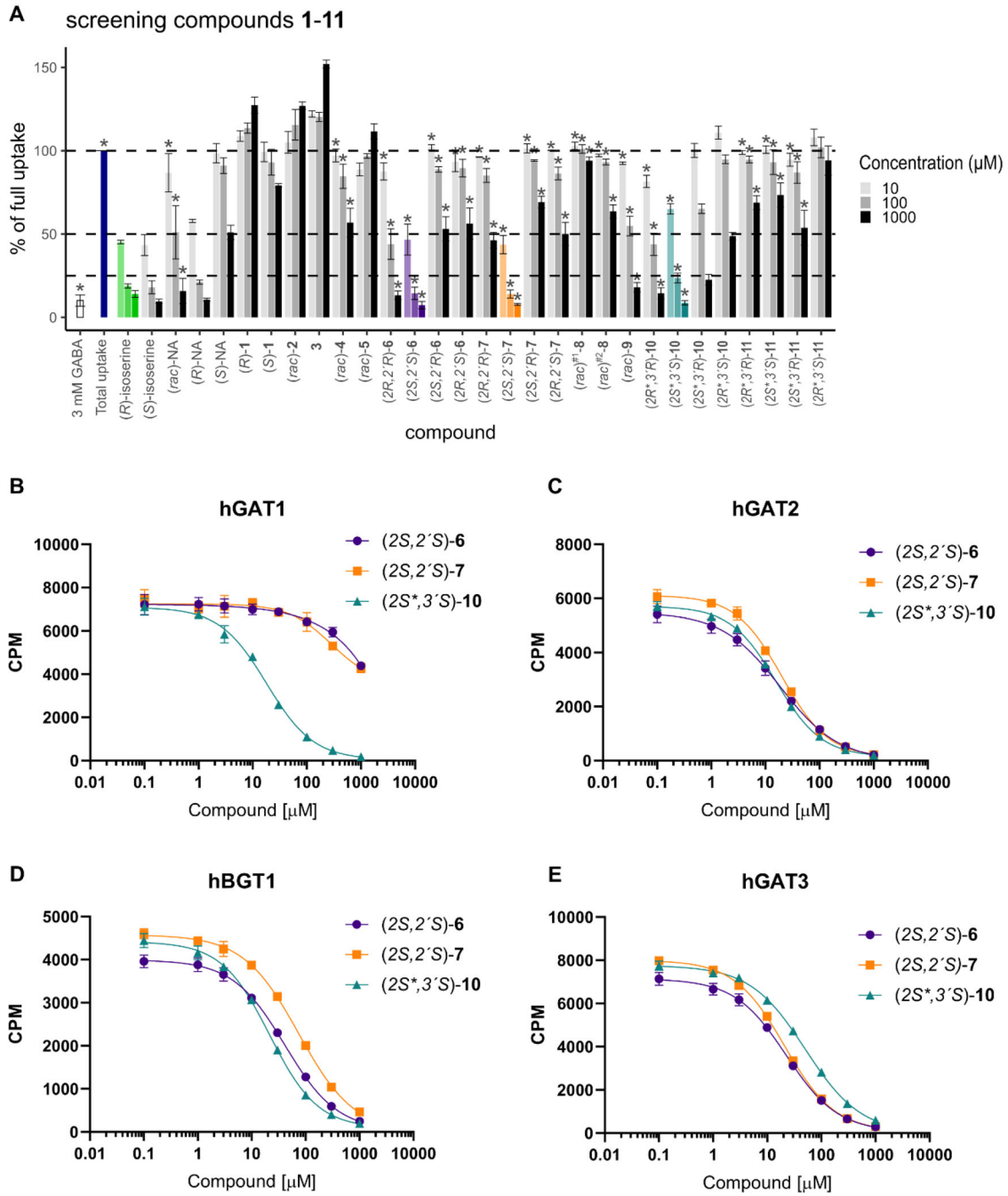

Fig. 3 **A** Screening of **1–11** in a [^{3}H]GABA uptake assay at hGAT3 transiently expressed in tsA201 cells. Compounds were tested at 10, 100 and 1000 µM. Data are normalized to 100% [^{3}H]GABA uptake and presented as the mean of residual [^{3}H]GABA uptake activity. Error bars indicate either the standard deviation of the mean (SD) for data points with $n = 1$ (three technical replicates) or standard error of the mean (SEM) for data points with $n = 2$ (indicated with "*"). Although the authors consider $n = 1$ sufficient for screening, several compounds were in fact tested in two independent experiments and, hence, those data are included. Concentration-response curves of (2*S*,2´*S*)-**6**, (2*S*,2´*S*)-**7** and (2*S**,3´*S*)-**10** at (**B**) hGAT1, (**C**) hGAT2, (**D**) hBGT1 and (**E**) hGAT3 transiently expressed in tsA201 cells. Curves were obtained via the [^{3}H]GABA uptake assay. Data shown are from one representative curve of two independent experiments in three technical replicates (error bars as SD). Average IC_{50} values are presented in Table 1. CPM counts per minute

racemic mixture of (2*S*,2´*S*)/(2*R*,2´*R*)-**7** previously reported as a mGAT4 inhibitor (14 µM) [29].

The conformationally locked (2*S*,2´*S*)-**6** and (2*S*,2´*S*)-**7** mimic the bioactive conformation of (*S*)-isoserine. The IC_{50} values are comparable but not superior to that of (*S*)-isoserine plausibly because some extent of flexibility might be beneficial for reaching the orthosteric binding site of the transporter.

Table 1 Functional activity and subtype selectivity of (2*S*,2´*S*)-**6**, (2*S*,2´*S*)-**7** and (2*S**,3´*S*)-**10**

	IC_{50} (μM) ($pIC_{50} \pm SEM$)[a]					K_i (μM)[b]
	hGAT3	hGAT1	hGAT2	hBGT1	hTauT	$GABA_A$Rs
(*S*)-**isoserine***	6.7	>1000	7.4	193.6	32.0	>1000
(2*S*,2´*S*)-**6**	19.0 (4.7 ± 0.08)	>1000	18.5 (4.7 ± 0.004)	54.0 (4.3 ± 0.10)	≥1000	>100
(2*S*,2´*S*)-**7**	17.7 (4.8 ± 0.08)	>1000	18.7 (4.7 ± 0.03)	82.2 (4.1 ± 0.04)	>100	>100
(2*S**,3´*S*)-**10**	41.9 (4.4 ± 0.09)	21.9 (4.7 ± 0.08)	16.6 (4.8 ± 0.06)	24.5 (4.6 ± 0.05)	–	–

[a]Concentration-response curves for (2*S*,2´*S*)-**6**, (2*S*,2´*S*)-**7** and (2*S**,3´*S*)-**10** at hGAT1-3 and hBGT1 were obtained with [^{3}H]GABA uptake assays in tsA201 cells transiently expressing hGATs (see Fig. 3B–E for full curves). (2*S*,2´*S*)-**6** and (2*S*,2´*S*)-**7** were also tested at 10, 100 and 1000 μM concentrations at hTauT and IC_{50} values were estimated (see Supplementary Fig. S1)

[b]Native $GABA_A$R affinities (K_i) were obtained from a [^{3}H]muscimol binding assay in rat cortical synaptic membranes as previously described [54].
*Data taken from Lie et al. [17]

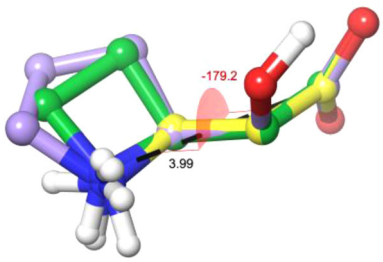

Fig. 4 Overlay between the most stable conformers of (2*S*,2´*S*)-**6** (green), (2*S*,2´*S*)-**7** (pink), and (*S*)-isoserine (yellow)

In order to visualize the bioactive conformation of (*S*)-isoserine, a conformational search of (2*S*,2´*S*)-**6** and (2*S*,2´*S*)-**7** was performed in water, using the Schrödinger Macromodel module [42]. The best scored conformers of (2*S*,2´*S*)-**6** and of (2*S*,2´*S*)-**7** were 12 and 7 KJ/mol, respectively, more energetically favorable than the second best scored conformations. Furthermore, those conformations displayed very good functional group alignment compared to the extended conformation of (*S*)-isoserine, with a 180° dihedral angle and 4 Å distance between the carboxylic acid and amino functionality (Fig. 4).

In the last series of unsubstituted compounds **9**–**11**, the nitrogen was moved from the β- to the γ- position, to better mimic the structure of GABA. Coherently with our design, Andreß et al. reported α-hydroxy-GABA (flexible analog of **9**–**11**) as a non-selective mGAT1/3/4 inhibitor [18]. Only the pyrrolidine-based diastereoisomer (2*S**,3´*S*)-**10** showed similar hGAT3 inhibition as (*S*)-isoserine (51 μM), confirming hGAT3 to be highly sensitive to stereochemical modifications.

Subtype selectivity and intrinsic activity of (2*S*,2´*S*)-6, (2*S*,2´*S*)-7 and (2*S**,3´*S*)-10

To determine the impact of conformational restriction of (*S*)-isoserine on subtype-selectivity, compounds with mid micromolar IC_{50} values at GAT3 (2*S*,2´*S*)-**6**, (2*S*,2´*S*)-**7** and (2*S**,3´*S*)-**10** were profiled in the [^{3}H]GABA uptake inhibition assay at tsA201 cells transiently expressing GAT1, GAT2 and BGT1 (Fig. 3B–E and Table 1). Similar to (*S*)-isoserine, (2*S*,2´*S*)-**6** and (2*S*,2´*S*)-**7** were GAT3-selective vs. GAT1 (>43× and 14× higher potency respectively), while displaying only minimal preference for hGAT3 over hBGT1 (2–3×) and no selectivity over hGAT2. Although no novel hGAT3 selective compound was identified, this subtype selectivity profile holds promise for selective modulation of tonic inhibition [15, 43, 44]. On the other hand, (2*S**,3´*S*)-**10** displayed very similar potency at all the four subtypes, probably due to higher structural similarity to GABA than (*S*)-isoserine, and could be further considered as a building block for the development of inhibitors of other GATs. In order to determine whether (2*S*,2´*S*)-**6** and (2*S*,2´*S*)-**7** are substrates at GAT3, and to confirm their expected preferential activity for GAT3 over GAT1 in a different assay system, they were assessed in the FLIPR® membrane potential (FMP) assay as previously described [24]. At GAT3, both compounds showed a concentration-dependent change in fluorescent signal (ΔFU) with an estimated EC_{50} value below 10 μM, when compared to max (100 μM) GABA (Fig. 5). At GAT1, a concentration-dependent change of the fluorescence signal was also observed for both compounds, however with a clearly reduced activity (no activity at 10 μM and an estimated EC_{50} value well above 100 μM). This shows that (2*S*,2´*S*)-**6** and (2*S*,2´*S*)-**7** are substrates with ~10–100 times preference for hGAT3 over hGAT1, and can therefore be classified as GAT3-preferring substrate inhibitors.

Additional off-target profiling of (2*S*,2´*S*)-6/(2*S*,2´*S*)-7

Given the pronounced activity of (*S*)-isoserine at TauT, a potential confounder in the analysis of in vivo results, we also evaluated the activity of (2*S*,2´*S*)-**6**, (2*S*,2´*S*)-**7** at TauT and $GABA_A$Rs. TauT activity was tested for the

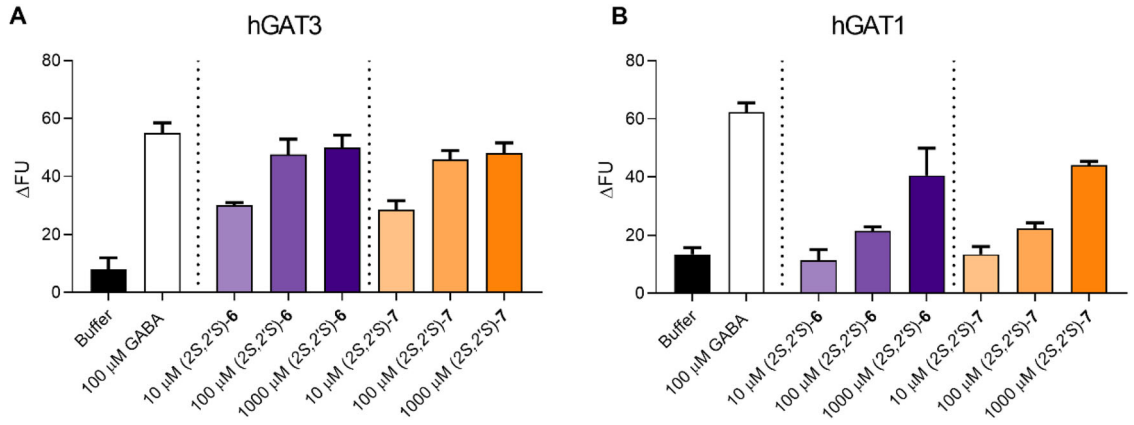

Fig. 5 Pharmacological evaluation of (2*S*,2´*S*)-**6** and (2*S*,2´*S*)-**7** at (**A**) hGAT3 and (**B**) hGAT1 in the FMP assay. The transporters were transiently expressed in tsA201 cells. The change in fluorescence signal (ΔFU) reflects a relative change in membrane potential and is determined in response to increasing concentration of compound. Data shown are a single representative experiment of two independent experiments and show clear substrate activity of (2*S*,2´*S*)-**6** and (2*S*,2´*S*)-**7** at hGAT3 and to a smaller extent at hGAT1. Error bars show SD of three technical replicates

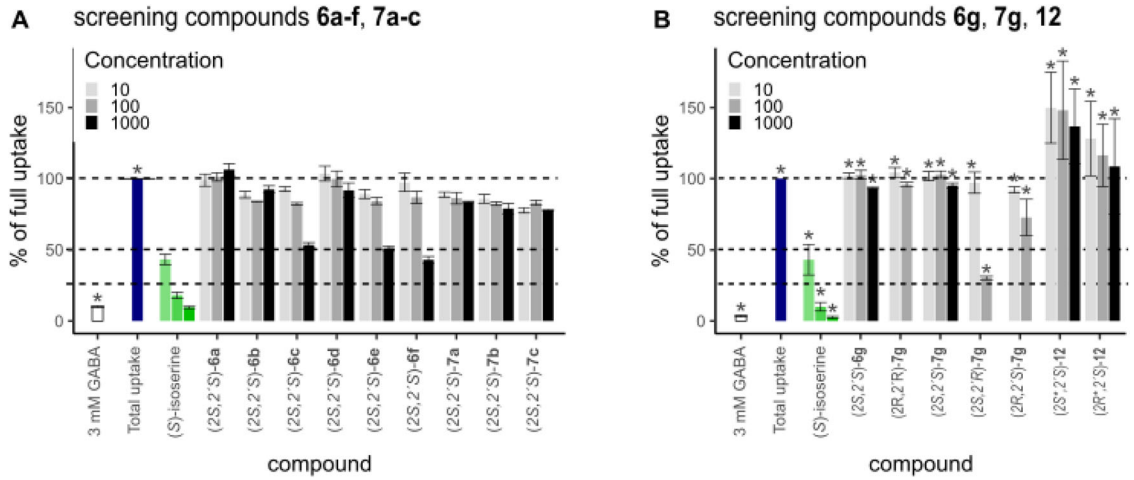

Fig. 6 Screening of (2*S*,2´*S*)-**6a–g**, (2*S*,2´*S*)-**7a–c**, **12** and **7g** in a [^{3}H] GABA uptake assay at hGAT3 (**A**) transiently expressed in tsA201 cells or (**B**) stably expressed in CHO cells. Compounds were tested at 10, 100 and 1000 µM. Data are normalized to 100% [^{3}H] GABA uptake and presented as the mean of residual [^{3}H]GABA uptake activity. Error bars indicate either SD for data points with $n = 1$ or SEM for data points with $n = 2$ (indicated with "*"), all from three technical replicates. Although the authors consider $n = 1$ sufficient for screening, several compounds were in fact tested in two independent experiments and, hence, those data are included

compounds in a [^{3}H]taurine uptake inhibition assay using hTauT transiently expressed in tsA201 cells. Affinity for $GABA_A$Rs was tested in the [^{3}H]muscimol binding assay using a rat cortical membrane preparation (Table 1 and Supplementary Fig. S1). Confirming the design rationale, conformational constrain of (*S*)-isoserine into the locked structures of (2*S*,2´*S*)-**6**, (2*S*,2´*S*)-**7** markedly reduced inhibition of TauT (~6 and 53 times preference for at hGAT3, respectively), and did not introduce affinity at native $GABA_A$Rs. Especially the absence of activity at TauT highlights these compounds as superior tool compounds over (*S*)-isoserine for native conditions.

Impact of *N*- and α-substitution on hGAT3 activity: screening of (2*S*,2´*S*)-6a–g, (2*S*,2´*S*)-7a–c, 12 and 7g at hGAT3

Exactly as described above, compounds (2*S*,2´*S*)-**6a–g**, (2*S*,2´*S*)-**7a–c**, **12** and **7g** were screened in a [^{3}H]GABA uptake inhibition assay (Fig. 6). Of the 16 compounds tested, only (2*S*,2´*R*)-**7g** displayed significant inhibition at hGAT3 (30% residual activity at 100 µM).

α-Methylation of (2*S*,2´*S*)-**6** resulted in the inactive compounds (2*S**,2´*S*)-**12** and (2*R**,2´*S*)-**12**, indicating very limited space in the binding pocket. None of the analogs (2*S*,2´*S*)-**6a–f**–(2*S*,2´*S*)-**7a–c** had any appreciable

inhibitory activity at hGAT3 at 100 µM (less than 25% inhibition). Considering, that the approach taken was successful for investigating structural determinants of ATPCA for hBGT1 activity but unsuccessful when applied to our best performing hGAT3 inhibitors, these results also suggest that the hGAT3 binding site is less permissive than hBGT1. Introduction of a (*E*)-4,4,4-tris(4-methoxyphenyl)but-2-en-1-yl substituent at the nitrogen of (2*S*,2´*S*)-**6** and (2*S*,2´*S*)-**7** provided (2*S*,2´*S*)-**6g** and (2*S*,2´*S*)-**7g** [29, 30]. Based on the structural similarity of (2*S*,2´*S*)-**7g** with (2*S*,2´*S*)/(2*R*,2´*R*)-**TS1**, we expected both (2*S*,2´*S*)-**6g** and (2*S*,2´*S*)-**7g** to display similar or improved IC_{50} values compared to their unsubstituted counterparts (2*S*,2´*S*)-**6** and (2*S*,2´*S*)-**7**. Instead, they did not display any hGAT3 inhibition at 100 µM. According to the hypothesis formulated by Wein et al., small and large binders of mGAT1 have different binding modes [26]. Cyclic amino acid-based inhibitors such as (*R*)-nipecotic acid perfectly fit the mGAT1 orthosteric binding site in the closed transporter conformation, with the nitrogen pointing toward the intracellular side of the transporter. Instead, *N*-substituents impose a 180° rotation of the cyclic amino acid moiety, resulting in a binding mode in which the nitrogen is positioned toward the extracellular vestibule, where the lipophilic bulk is accommodated. Similarly, we have also previously proposed that the small amino acid-like BGT1 substrate ATPCA binds the orthosteric binding site with the nitrogen positioned downwards, while its *N*-substituted derivatives must undergo a conformational change to fit the pocket in a bent conformation, and result in inactive compounds if this conformational change is not allowed by reduced flexibility [27]. Inactivity of (2*S*,2´*S*)-**6g** and (2*S*,2´*S*)-**7g** suggests these hypotheses to be translatable to hGAT3: the different binding mode imposed by the bulky lipophilic substituent would cause a disruption of the sharp stereochemical requirements for hGAT3 inhibition. To further support this hypothesis, (2*R*,2´*R*)-, (2*R*,2´*S*)- and (2*S*,2´*R*)-**7g** were synthesized. As mentioned, among these, only (2*S*,2´*R*)-**7g** displayed a significant inhibition of [^{3}H]GABA uptake (70% inhibition at 100 µM or 30% residual activity), confirming: (1) different stereochemical requirements between small amino acid-based and bulky *N*-substituted hGAT3 inhibitors, possibly due to different binding modes at hGAT3; (2) the low relevance of the amino acid structure when a lipophilic bulky substituent is introduced; (3) the possibility of transforming very weak GAT3 inhibitor (such as (2*S*,2´*R*)-**7**, no inhibition at 100 µM) into a moderate inhibitor (such as (2*S*,2´*R*)-**7g**, 70% inhibition at 100 µM) by introducing the appropriate lipophilic bulky substituent, as also described for GAT1 by Wein et al. [26].

Conclusion

In summary, to understand the structural determinants of isoserine for GAT3 inhibition we have performed a systematic investigation of the structural and stereochemical requirements for hGAT3 inhibition of locked analogs of (*S*)-isoserine. Four series of conformationally restricted compounds were synthesized as single stereoisomers for the majority: three exploiting different rigidification patterns (connecting the nitrogen with the α-hydroxy, with the α-carbon or with the β-carbon), and the fourth by repositioning the nitrogen from the β- to the γ-carbon.

From this study the following messages can be drawn. (1) Compared to (*S*)-isoserine, two novel GAT3 ligands (2*S*,2´*S*)-**6** and (2*S*,2´*S*)-**7** that have a similar GAT subtype profile but significantly improved selectivity vs. TauT (at least 6× and 53×, respectively) have been developed. (2) Our study unravels key structural and stereochemical features required for hydroxylated amino acids to inhibit GAT3. (3) We discovered a strikingly different stereochemical prerequisite between *N*-substituted GAT3 inhibitors and their unsubstituted analogs suggesting different binding modes. All in all, observations instrumental for future ligand design to target GAT3-mediated pathologies.

Furthermore, compounds like (2*S*,2´*S*)-**6** and (2*S*,2´*S*)-**7** could be valuable to validate the proposed GAT3-mediated effect of (*S*)-isoserine in e.g., functional recovery after stroke [17], and as such help corroborate the relevance of targeting GAT3 and tonic inhibition in relevant brain pathologies.

Experimental

Chemistry

General procedures

All reagents were purchased from commercial suppliers and used without further purification. Standard HPLC-grade quality solvents were used. Anhydrous THF, DCM, and DMF were obtained from a Glass Contour Solvent System (SG Water USA). Anhydrous MeOH was obtained by distillation over CaH_2 and stored over activated 3 Å molecular sieves for a minimum of 24 h (according to standard protocols). Et_3N and pyridine were kept dry by storage over activated 3 Å molecular sieves. Thin-layer chromatography (TLC) were performed using Merck aluminum sheets covered with silica gel C-60 F254. Visualization of TLC plates was performed using UV light (254 nm), $KMnO_4$ stain, or *p*-anisaldehyde stain prepared according to standard procedures. Flash column chromatography was performed using glass columns packed with Merck Geduran Si 60

(0.040–0.063 mm) as a stationary phase, or with a Combi Flash NextGen 300+ system (Teledyne) on RediSep Gold® silica gel flash columns of the appropriate size. Eluent systems are reported as volume ratios, and R_f value are specified under each protocol. 1D and 2D NMR spectra were acquired using a Bruker Avance II equipped with a 5 mm broad band probe (BBFO) operating at 400 MHz for ^{1}H NMR and 101 MHz for ^{13}C NMR or a Bruker Avance III HD equipped with a cryogenically cooled 5 mm dual probe optimized for ^{13}C and ^{1}H NMR operating at 600 MHz for ^{1}H NMR and 151 MHz for ^{13}C NMR. HSQC, HMBC, and ROESY experiments were used to support analyses when ^{1}H NMR, ^{13}C NMR, and COSY were inadequate. Chemical shifts (δ) are reported in ppm downfield from TMS ($\delta = 0$) using either the solvent resonance as the internal standard ($CDCl_3$, ^{1}H: 7.26 ppm, ^{13}C: 77.16 ppm; DMSO-*d*6, ^{1}H: 2.50 ppm, ^{13}C: 39.52 ppm; MeOD, ^{1}H: 3.31 ppm, ^{13}C: 49.00 ppm; D_2O, ^{1}H: 4.79 ppm) or 3-(trimethylsilyl)propionic-2,2,3,3-*d*4 acid sodium salt (TMSP, ^{13}C: 0 ppm). Coupling constants (*J*) are reported in Hz, and the field is reported in each case. Multiplicities are reported as singlet (s), broad singlet (bs), doublet (d), doublet of doublets (dd), doublet of triplets (dt), doublet of doublet of doublets (ddd), doublet of doublet of triplets (ddt), triplet (t), triplet of doublets (td), quartet (q), pentet (p), septet (sep), and multiplet (m). Mass spectrometric data was recorded using either a LC-MS system built from an Agilent 1200 series solvent delivery system equipped with an autoinjector coupled to a DAD and an Agilent 6130A series quadrupole electrospray ionization detector or a Waters Aquity UPLC-MS equipped with a dual-wavelength PDA (214 and 254 nm) combined with electrospray ionization. Gradients of H_2O/MeCN/HCOOH (95:5:0.1) (solvent A) and MeCN/HCOOH (100:0.1) (solvent B) were employed. Purity was assessed by analytical HPLC on an UltiMate HPLC system (Thermo Scientific) consisting of an LPG-3400A pump (1 ml/min), a WPS-3000SL autosampler, and a DAD-3000D diode array detector using a Gemini-NX C18 column (4.6 × 250 mm, 3 µm, 110 Å); gradient elution was 0 to 100% B (MeCN/H_2O/TFA, 90:10:0.1) in solvent A (H_2O/TFA, 100:0.1) over 20 min. Data were acquired and processed using Chromeleon Software v. 6.80. For final compounds (**6a**–**g**, **7a**–**c**, **g**) analytical purity is ≥95%; retention times (t_R) are indicated. Chiral analytical HPLC was performed using an Hitachi 7000 series HPLC apparatus consisting of a D-7000 interface unit, an L-7100 pump (0.8 ml/min), a L-7200 autosampler, a L-7400 UV variable detector (detection at 190 nm), using a Astec Chirobiotic T column (5 µm, 4.6 × 250 mm); isocratic elution with 60% solvent A (milliQ water) and 40% solvent B (methanol) was performed. Enantiomeric excesses (ee) of compounds (2*S*,2´*S*)-**6** and (2*S*,2´*S*)-**7** were higher than 99% and retention times (Rt) are reported. Preparative HPLC purification was carried out on a Dionex Ultimate 3000 HLPC system consisting of an LPG-3200BX pump (20 ml/min), a Rheodyne 9725i injector, a 10 ml loop, an MWD-3000SD detector (200, 210, 254, and 281 nm), and an AFC-3000SD automated fraction collector using a Gemini-NX C18 column (21.2 × 250 mm, 5 µm, 110 Å). Solvent A (H_2O/TFA, 100:0.1) and solvent B (MeCN/H_2O/TFA, 90:10:0.1) were utilized. Unless specified otherwise, a gradient elution from 0% B to 100% B was used, over 20 min. Data were acquired and processed using Chromeleon Software v.6.80. Mosher analysis of intermediates (2*S*,2´*S*)-**21** and (2*S*,2´*S*)-**22** was performed according to protocols reported in literature.

Method A: general procedure for the preparation of compounds 15, (*rac*)-16, and stereoisomers of 21–23, 29–31, 35

The appropriate aldehyde or ketone (5.02 mmol, 1 eq) was dissolved in diethyl ether (5 ml). A solution of $NaHSO_3$ (1.2 eq) in deionized water (10 ml) was added. After stirring for 15 min, KCN (1.5 eq) was carefully added, and the reaction mixture was stirred at room temperature overnight. The reaction mixture was diluted with diethyl ether (30 ml), the phases separated, and the water layer was extracted with diethyl ether (3 × 10 ml). The combined organic phases were dried over anhydrous sodium sulfate, filtered, and the solvent was evaporated under reduced pressure. The crude was purified by silica gel flash column chromatography as specified, providing the desired compounds **15**, (*rac*)-**16**, and stereoisomers of **21**–**23**, **29**–**31** and **35** in variable yields (11–90%).

Method B: general procedure for the preparation of compounds 3, (*rac*)-4, and stereoisomers of 6–12

The α-hydroxynitrile of interest (0.40 mmol) was suspended in HCl 4 M (1 ml) and heated to 85 °C overnight. Upon completion, the solution was cooled to rt, the volatiles were removed under reduced pressure and the residue was desalted by ion exchange chromatography (5 M NH_{3aq}). The crude purified as specified, providing the desired products **3**, (*rac*)-**4**, and stereoisomers of **6**–**12** as off-white solids in variable yields (17–75%).

Method C: general procedure for the preparation of stereoisomers of compounds 18, 27, 28

The appropriate primary alcohol (25.8 mmol, 1 eq) was dissolved in DCM (50 ml), and trichloroisocyanuric acid (1.05 eq) was added portion-wise. Upon cooling to 0 °C, TEMPO (0.01 eq) was slowly added. The reaction was allowed to warm at rt and stirred for 15 min at rt. Upon

completion, the mixture was filtered over celite®, and the resulting solution was washed with a saturated solution of Na_2CO_3 (3 × 15 ml), HCl 1 M (3 × 15 ml), and brine (10 ml). The organic phase was dried over anhydrous sodium sulfate, filtered, the solvents were removed under reduced pressure. The crude was purified by silica gel flash column chromatography when specified, providing the desired stereoisomers of **18**, **27** and **28** in moderate to excellent yields (42–95%).

Method D: general procedure for the preparation of compounds (2*S*,2´*S*)-6a–f and (2*S*,2´*S*)-7a–c

In an oven-dried tube under inert atmosphere, intermediate (2*S*,2´*S*)-**6** or (2*S*,2´*S*)-**7** (0.31 mmol, 1 eq), the appropriate aromatic aldehyde (1 eq) and $NaBH_3CN$ (1 eq) were suspended in dry methanol (2 ml). The reaction mixture was stirred at 60 °C overnight. Upon cooling, the mixture was quenched with 2 ml water and diluted with methanol until a clear solution was formed. Purification by preparative HPLC provided the desired compounds (2*S*,2´*S*)-**6a–f** and (2*S*,2´*S*)-**7a–c** in moderate to good yields (31–89%).

Method E: general procedure for the preparation of compounds (2*S*,2´*S*)-36 and stereoisomers of 37

To an ice-cooled stirred solution of the carboxylic acid (2*S*,2´*S*)-**6** or the appropriate stereoisomer of **7** (0.90 mmol, 1 eq) in methanol (2.5 ml), thionyl chloride (4 eq) was carefully added dropwise over 5 min, and the reaction mixture was left stirring at rt overnight. The volatiles were evaporated under reduced pressure, and the residue was diluted with EtOAc (3 ml), cooled to 0 °C, and water (3 ml) was added. The pH of the water layer was adjusted to 10 by dropwise adding a 4 M solution of NaOH. The two phases were separated and water layer was extracted with EtOAc (3 × 10 ml). The combined organic layers were dried over anhydrous sodium sulfate, filtered, and the solvents were evaporated under reduced pressure providing the desired compound (2*S*,2´*S*)-**36** and the stereoisomers of **37** in very good yields (75–92%).

Method F: general procedure for the preparation of compounds (2*S*,2´*S*)-38g and stereoisomers of 39g

To a flame-dried two-neck flask under inert atmosphere, the appropriate steroisomer of intermediate **36** or **37** (0.32 mmol, 1 eq) was dissolved in 3 ml of acetone/DMF/ACN 1:1:1. K_2CO_3 (3 eq) and KI (0.1 eq) were added, and the suspension was stirred for 30 min. Afterwards, (*E*)-4,4',4''-(4-bromobut-2-ene-1,1,1-triyl)tris(methoxybenzene) **40** (1.3 eq) was added, and the reaction mixture was stirred at rt overnight in the dark. Upon completion, 10 ml of EtOAc were added, the resulting suspension was filtered and the filtrate was evaporated under reduced pressure, providing a crude that was purified by preparative HPLC. The desired compound (2*S*,2´*S*)-**38g** and the stereoisomers of **39g** were obtained in low yields (14–37%).

Method G: general procedure for the preparation of compounds (2*S*,2´*S*)-6g and stereoisomers of 7g

To the methyl ester (2*S*,2´*S*)-**38g** and or to the appropriate steroisomer of **39g** (0.07 mmol, 1 eq), a 1:1 mixture of LiOH 2 M in water/dioxane (1 ml) was added. The reaction mixture was stirred for 2 h at rt and then dioxane was evaporated under reduced pressure. The resulting crude was purified by preparative HPLC, providing the desired compound (2*S*,2´*S*)-**6g** and the stereoisomers of **7g** in moderate yields (32–74%).

Synthesis of tert-butyl 3-cyano-3-hydroxyazetidine-1-carboxylate (15) Obtained from of *tert*-butyl 3-oxoazetidine-1-carboxylate **13** (500 mg, 2.90 mmol), according to Method A as a white solid in 90% yield. ^{1}H NMR (400 MHz, $CDCl_3$) δ 4.38 (d, $J = 9.6$ Hz, 2H), 4.08 (d, $J = 9.6$ Hz, 2H), 1.45 (s, 9H). ^{13}C NMR (151 MHz, $CDCl_3$) δ 156.0, 119.2, 81.5, 60.6, 28.4. R_f (1:1 heptane/EtOAc) = 0.50 R_t (LC-MS) = 3.651 min. LC-MS (ESI): *m/z* calcd. for $C_5H_7N_2O_3$ $[M + H\text{-}tBu]^+ = 143.12$, found 143.1.

Synthesis of 3-carboxy-3-hydroxyazetidine hydrochloride (3) Obtained from *tert*-butyl 3-cyano-3-hydroxyazetidine-1-carboxylate **15** (100 mg, 0.50 mmol), according to Method B. The residue was taken in HCl 1 M, dried, and the solid was crystallized from isopropanol in 21% yield. R_t (LC-MS) = 0.492 min. LC-MS (ESI): *m/z* calcd. for $C_4H_7NO_3^+$ $[M + H]^+ = 118.05$, found 118.0. ^{1}H NMR (600 MHz, MeOD) δ 4.43 (d, $J = 11.9$ Hz, 2H), 4.08 (d, $J = 11.9$ Hz, 2H). ^{13}C NMR (151 MHz, MeOD) δ 173.6, 71.9, 58.7.

Synthesis of (*rac*)-tert-butyl 3-cyano-3-hydroxypyrrolidine-1-carboxylate ((*rac*)-16) Obtained from of *tert*-butyl 3-oxopyrrolidine-1-carboxylate **14** (1.00 g, 5.4 mmol), according to Method A as a white solid in 61% yield. R_f (1:1 *n*-heptane/EtOAc) = 0.63. R_t (LC-MS) = 3.597 min. LC-MS (ESI): *m/z* calcd. for $C_6H_9N_2O_3$ $[M + H\text{-}tBu]^+ = 157.06$, found 157.1. ^{1}H NMR (600 MHz, $CDCl_3$) δ 4.02 (bs, 1H), 3.80–3.61 (m, 3H), 3.61–3.51 (m, 1H), 2.37–2.30 (m, 2H), 1.47 (s, 9H). ^{13}C NMR (151 MHz, $CDCl_3$) δ 154.6, 154.3, 119.6, 81.0, 80.9, 70.8, 69.9, 57.8, 57.5, 44.0, 43.6, 38.7, 38.4, 28.6. ^{1}H- and ^{13}C-NMR data in accordance with literature [45].

Synthesis of (*rac*)-3-hydroxypyrrolidine-3-carboxylic acid ((*rac*)-4) Obtained from (*rac*)-*tert*-butyl 3-cyano-3-hydroxypyrrolidine-1-carboxylate (*rac*)-**16**. (200 mg, 0.94 mmol), according to Method B. The crude was dissolved in water, precipitated with acetone at 0 °C and filtered, providing the desired compound as a off-white solid in 75% yield. R_t (LC-MS) = 0.474 min. LC-MS (ESI): *m/z* calcd. for $C_5H_{10}NO_3^+$ $[M + H]^+ = 132.07$, found 132.1. ^{1}H NMR (600 MHz, D_2O) δ 3.65–3.59 (m, 2H), 3.54 (ddd, $J = 11.7$, 9.6, 7.5 Hz, 1H), 3.39 (dd, $J = 12.3$, 1.7 Hz, 1H), 2.42 (dt, $J = 13.8$, 9.6 Hz, 1H), 2.19 (dddd, $J = 13.8$, 7.5, 3.6, 1.7 Hz, 1H). ^{13}C NMR (151 MHz, D_2O) δ 180.5, 83.5, 58.2, 47.6, 39.5.

Synthesis of tert-butyl (*S*)-2-formylazetidine-1-carboxylate ((*S*)-18) Obtained from *tert*-butyl (*S*)-2-(hydroxymethyl) azetidine-1-carboxylate (*S*)-**17** (900 mg, 4.81 mmol), according to Method C, as an oil in 48% yield after silica gel flash column chromatography (gradient from *n*-heptane to *n*-heptane/THF 1:1). R_f (2:1 *n*-heptane/THF) = 0.29. R_t (LC-MS) = 4.617 min. LC-MS (ESI): *m/z* calcd. for $C_{18}H_{31}N_2O_6$ $[2\,M + H]^+ = 371.22$, found 371.2. ^{1}H NMR (400 MHz, $CDCl_3$) δ 9.79 (s, 1H), 4.59 (t, $J = 7.6$ Hz, 1H), 4.03–3.87 (m, 2H), 2.52–2.37 (m, 1H), 2.36–2.19 (m, 1H), 1.44 (s, 9H). ^{1}H-NMR data in accordance with literature [46].

Synthesis of tert-butyl (*R*)-2-formylazetidine-1-carboxylate ((*R*)-18) Obtained from *tert*-butyl (*R*)-2-(hydroxymethyl) azetidine-1-carboxylate (*R*)-**17** (1.00 g, 5.30 mmol), according to Method C, as an oil in 42% yield after silica gel flash column chromatography (gradient from *n*-heptane to *n*-heptane/THF 1:1). TLC, LC-MS, ^{1}H NMR data as for (*S*)-**18**.

Synthesis of tert-butyl (*S*)-2-((*S*)-cyano(hydroxy)methyl)azetidine-1-carboxylate (2*S*,2′*S*)-21 and of (*S*)-2-((*R*)-cyano(hydroxy)methyl)azetidine-1-carboxylate (2*R*,2′*S*)-21 Obtained from *tert*-butyl (*S*)-2-formylazetidine-1-carboxylate (*S*)-**18** (570 mg, 3.08 mmol), according to Method A. Purification by silica gel flash column chromatography (gradient from DCM to DCM/ethyl acetate 9:1) allowed separation of the two diastereoisomers (2*S*,2′*S*)-**21** and (2*R*,2′*S*)-**21**. Diastereoisomer (2*S*,2′*S*)-**21** was obtained as a white solid in 48% yield. R_f (DCM/ethyl acetate 95:5) = 0.39. R_t (LC-MS) = 3.679 min. LC-MS (ESI): *m/z* calcd. for $C_6H_9N_2O_3$ $[M + H\text{-tBu}]^+ = 157.06$, found 157.1. ^{1}H NMR (400 MHz, $CDCl_3$) δ 6.25 (d, $J = 10.5$ Hz, 1H), 4.72–4.54 (m, 1H), 4.48 (dd, $J = 10.5$, 2.2 Hz, 1H), 4.04–3.84 (m, 2H), 2.43–2.26 (m, 1H), 2.25–2.08 (m, 1H), 1.47 (s, 9H). ^{13}C NMR (101 MHz, $CDCl_3$) δ 158.2, 117.6, 82.2, 66.7, 63.9, 47.3, 28.4, 18.2. Mosher analysis and ^{1}H NMR/conformational analysis determined (*S,S*) configuration for (2*S*,2′*S*)-**21**. Diastereoisomer (2*R*,2′*S*)-**21** was obtained as a white solid in 33% yield. R_f (DCM/ethyl acetate 95:5) = 0.21. R_t (LC-MS) = 3.523 min. LC-MS (ESI): *m/z* calcd. for $C_6H_9N_2O_3$ $[M + H\text{-tBu}]^+ = 157.06$, found 157.1. ^{1}H NMR (400 MHz, $CDCl_3$) δ 5.50 (bs, 1H), 4.64 (d, $J = 8.3$ Hz, 1H), 4.53 (td, $J = 8.3$, 6.6 Hz, 1H), 3.93 (td, $J = 8.7$, 7.2 Hz, 1H), 3.84 (td, $J = 8.7$, 4.7 Hz, 1H), 2.40 (dtd, $J = 12.0$, 8.7, 4.7 Hz, 1H), 2.21–2.06 (m, 1H), 1.46 (s, 9H). ^{13}C NMR (151 MHz, $CDCl_3$) δ 158.0, 117.0, 82.2, 66.5, 64.0, 46.9, 28.4, 18.5. ^{1}H NMR/conformational analysis determined (*R,S*) absolute configuration for (2*R*,2′*S*)-**21**.

Synthesis of tert-butyl (*R*)-2-((*R*)-cyano(hydroxy)methyl)azetidine-1-carboxylate (2*R*,2′*R*)-21 and of (*R*)-2-((*S*)-cyano(hydroxy)methyl)azetidine-1-carboxylate (2*S*,2′*R*)-21 Obtained from *tert*-butyl (*R*)-2-formylazetidine-1-carboxylate (*R*)-**18** (340 mg, 1.84 mmol), according to Method A. Purification by silica gel flash column chromatography (gradient from DCM to DCM/EtOAc 9:1) allowed separation of the two diastereoisomers (2*R*,2′*R*)-**21** and (2*S*,2′*R*)-**21**. Diastereoisomer (2*R*,2′*R*)-**21** was obtained as a white solid in 42% yield. TLC, LC-MS, ^{1}H NMR and ^{13}C NMR data as for (2*S*,2′*S*)-**21**, confirming (*R,R*) configuration for (2*R*,2′*R*)-**21**. Diastereoisomer (2*S*,2′*R*)-**21** was obtained as a white solid in 30% yield. TLC, LC-MS, ^{1}H NMR and ^{13}C NMR data as for (2*R*,2′*S*)-**21**, confirming (*S,R*) configuration of (2*S*,2′*R*)-**21**.

Synthesis of (*S*)-2-((*S*)-azetidin-2-yl)-2-hydroxyacetic acid (2*S*,2′*S*)-6 Obtained from *tert*-butyl (*S*)-2-((*S*)-cyano(hydroxy)methyl)azetidine-1-carboxylate (2*S*,2′*S*)-**21** (162 mg, 0.76 mmol), according to Method B. The residue was crystallized by water/ethanol, providing the desired compound (2*S*,2′*S*)-**6** in 53% yield. R_t (LC-MS) = 0.516 min. LC-MS (ESI): *m/z* calcd. for $C_5H_{10}NO_3^+$ $[M + H]^+ = 132.07$, found 132.1. HRMS (MALDI) *m/z* calcd. for $C_5H_{10}NO_3$ $[M + H]^+ = 132.0661$, found: 132.06553. R_t (chiral HPLC) = 7.19 min. ^{1}H NMR (600 MHz, D_2O) δ 4.85 (dddd, $J = 8.9$, 8.1, 4.0, 0.8 Hz, 1H), 4.34 (d, $J = 4.0$ Hz, 1H), 4.09 (ddd, $J = 10.6$, 9.5, 8.3 Hz, 1H), 3.93 (tdd, $J = 10.6$, 6.0, 0.8 Hz, 1H), 2.60–2.51 (m, 1H), 2.49–2.42 (m, 1H). ^{13}C NMR (151 MHz, D_2O) δ 178.6, 72.8, 64.6, 46.2, 21.7.

Synthesis of (*R*)-2-((*S*)-azetidin-2-yl)-2-hydroxyacetic acid (2*R*,2′*S*)-6 Obtained from *tert*-butyl (*S*)-2-((*R*)-cyano(hydroxy)methyl)azetidine-1-carboxylate (2*R*,2′*S*)-**21** (106 mg, 0.50 mmol), according to Method B. The residue was crystallized by water/ethanol, providing the desired compound (2*R*,2′*S*)-**6** in 42% yield. R_t (LC-MS) = 0.581 min. LC-MS (ESI): *m/z* calcd. for $C_5H_{10}NO_3^+$ $[M + H]^+ = 132.07$, found 132.0. ^{1}H NMR (600 MHz, D_2O) δ 4.82–4.79 (m, 1H), 4.26 (d, $J = 4.6$ Hz, 1H), 4.13 (qd, $J = 9.7$, 0.9 Hz, 1H), 3.91 (tdd, $J = 10.7$, 5.5, 0.9 Hz, 1H), 2.70–2.62 (m, 1H), 2.61–2.53 (m, 1H). ^{13}C NMR (151 MHz, D_2O) δ 178.9, 73.7, 65.0, 46.1, 24.1.

Synthesis of (*R*)-2-((*R*)-azetidin-2-yl)-2-hydroxyacetic acid (2*R*,2´*R*)-6 Obtained from *tert*-butyl (*R*)-2-((*R*)-cyano(hydroxy)methyl)azetidine-1-carboxylate (2*R*,2´*R*)-**21** (114 mg, 0.54 mmol), according to Method B. The residue was crystallized by water/ethanol, providing the desired compound (2*R*,2´*R*)-**6** in 47% yield. R_t (chiral HPLC) = 8.45 min. LC-MS, ^{1}H NMR and ^{13}C NMR data as for (2*S*,2´*S*)-**6**, confirming (*R,R*) configuration of (2*R*,2´*R*)-**6**.

Synthesis of (*S*)-2-((*R*)-azetidin-2-yl)-2-hydroxyacetic acid (2*S*,2´*R*)-6 Obtained from *tert*-butyl (*R*)-2-((*S*)-cyano(hydroxy)methyl)azetidine-1-carboxylate (2*S*,2´*R*)-**21** (117 mg, 0.55 mmol), according to Method B. The residue was crystallized by water/ethanol, providing the desired compound (2*S*,2´*R*)-**6** in 33% yield. LC-MS, ^{1}H NMR and ^{13}C NMR data as for (2*R*,2´*S*)-**6**, confirming (*S,R*) configuration of (2*S*,2´*R*)-**6**.

Synthesis of tert-butyl (*S*)-2-((*S*)-cyano(hydroxy)methyl)pyrrolidine-1-carboxylate (2*S*,2´*S*)-22 and of (*S*)-2-((*R*)-cyano(hydroxy)methyl)pyrrolidine-1-carboxylate (2*R*,2´*S*)-22 Obtained from *tert*-butyl (*S*)-2-formylpyrrolidine-1-carboxylate (*S*)-**19** (1.00 g, 5.02 mmol), according to Method A. Purification by silica gel flash column chromatography (gradient from DCM to DCM/EtOAc 9:1) allowed separation of the two diastereoisomers (2*S*,2´*S*)-**22** and (2*R*,2´*S*)-**22**. Diastereoisomer (2*S*,2´*S*)-**22** was obtained as a white solid in 31% yield. R_f (DCM/EtOAc 95:5) = 0.56. R_t (LC-MS) = 3.863 min. LC-MS (ESI): *m/z* calcd. for $C_7H_{10}N_2O_3$ $[M\text{-}tBu+H]^+ = 171.08$, found 171.0. ^{1}H NMR (400 MHz, $CDCl_3$) δ 7.07 (d, $J = 9.2$ Hz, 1H), 4.50 (d, $J = 9.2$ Hz, 1H), 4.11 (t, $J = 7.4$ Hz, 1H), 3.64–3.55 (m, 1H), 3.51–3.39 (m, 1H), 2.30–2.16 (m, 1H), 2.10–1.99 (m, 1H), 1.88–1.68 (m, 2H), 1.50 (s, 9H). ^{13}C NMR (151 MHz, $CDCl_3$) δ 158.1, 118.4, 82.2, 67.9, 62.0, 48.4, 29.2, 28.5, 23.8. Mosher analysis determined (*S,S*) configuration for (2*S*,2´*S*)-**22**. Diastereoisomer (2*R*,2´*S*)-**22** was obtained as a white solid in 46% yield. R_f (DCM/EtOAc 95:5) = 0.34. R_t (LC-MS) = 3.789 min. LC-MS (ESI): *m/z* calcd. for $C_7H_{10}N_2O_3$ $[M\text{-}tBu + H]^+ = 171.08$, found 171.0. ^{1}H NMR (600 MHz, $CDCl_3$) δ 5.74 (s, 1H), 4.45 (d, $J = 8.4$ Hz, 1H), 4.19 (t, $J = 8.4$ Hz, 1H), 3.53–3.42 (m, 1H), 3.42–3.34 (m, 1H), 2.25–2.15 (m, 1H), 2.00–1.84 (m, 3H), 1.47 (s, 9H). ^{13}C NMR (151 MHz, $CDCl_3$) δ 158.0, 118.9, 81.9, 66.7, 61.0, 47.9, 28.5, 28.5, 24.0. ^{1}H NMR analysis determined (*R,S*) absolute configuration for (2*R*,2´*S*)-**22**.

Synthesis of tert-butyl (*R*)-2-((*R*)-cyano(hydroxy)methyl)pyrrolidine-1-carboxylate (2*R*,2´*R*)-22 and of (*R*)-2-((*S*)-cyano(hydroxy)methyl)pyrrolidine-1-carboxylate (2*S*,2´*R*)-22 Obtained from tert-butyl (*R*)-2-formylpyrrolidine-1-carboxylate (*R*)-**19** (1.00 g, 5.02 mmol), according to Method A. Purification by silica gel flash column chromatography (gradient from DCM to DCM/EtOAc 9:1) allowed separation of the two diastereoisomers (2 *R*,2´*R*)-**22** and (2*S*,2´*R*)-**22**. Diastereoisomer (2*R*,2´*R*)-**22** was obtained as a white solid in 31% yield. TLC, LC-MS, ^{1}H NMR and ^{13}C NMR data as for (2*S*,2´*S*)-**22**, confirming (*R,R*) configuration of (2*R*,2´*R*)-**22**. Diastereoisomer (2*S*,2´*R*)-**22** was obtained as a white solid in 35% yield. TLC, LC-MS, ^{1}H NMR and ^{13}C NMR data as for (2*R*,2´*S*)-**22**, confirming (*S,R*) configuration of (2*S*,2´*R*)-**22**.

Synthesis of (*S*)-2-((*S*)-pyrrolidin-2-yl)-2-hydroxyacetic acid (2*S*,2´*S*)-7 Obtained from *tert*-butyl (*S*)-2-((*S*)-cyano(hydroxy)methyl)pyrrolidine-1-carboxylate (2*S*,2´*S*)-**22** (91 mg, 0.40 mmol), according to Method B. The residue was crystallized from ethanol, providing the desired compound (2*S*,2´*S*)-**7** in 38% yield. R_t (LC-MS) = 0.551 min. LC-MS (ESI): *m/z* calcd. for $C_6H_{12}NO_3^+$ $[M + H]^+ = 146.08$, found 146.1. HRMS (MALDI) *m/z* calcd. for $C_6H_{12}NO_3$ $[M + H]^+ = 146.0817$, found: 146.0811. R_t (chiral HPLC) = 8.30 min. ^{1}H NMR (600 MHz, D_2O) δ 4.33 (d, $J = 4.1$ Hz, 1H), 3.96 (ddd, $J = 9.5$, 7.3, 4.1 Hz, 1H), 3.38 (t, $J = 7.0$ Hz, 2H), 2.15–2.08 (m, 1H), 2.08–1.97 (m, 2H), 1.97–1.86 (m, 1H). ^{13}C NMR (151 MHz, D_2O) δ 179.7, 72.2, 64.6, 48.9, 26.7, 26.2.

Synthesis of (*S*)-2-((*S*)-pyrrolidin-2-yl)-2-hydroxyacetic acid (2*S*,2´*S*)-7-TFA Prepared by dissolving (2*S*,2´*S*)-**7** (10 mg, 0.07 mmol, 1 eq) in water (1 ml) and treating it with TFA (6 µl, 0.08 mmol, 1.2 eq) for 10 min at room temperature. Evaporation under reduced pressure and freeze drying provided the desired compound (2*S*,2´*S*)-**7**-TFA as a colorless oil in 77% yield. ^{1}H NMR (600 MHz, MeOD) δ 4.42 (d, $J = 4.3$ Hz, 1H), 4.02–3.88 (m, 1H), 3.34–3.31 (m, 2H), 2.16–1.92 (m, 4H). ^{13}C NMR (151 MHz, MeOD) δ 174.5, 163.07 (q, $J = 34.0$ Hz), 117.4 (q, $J = 292.2$ Hz), 69.7, 62.5, 47.3, 25.5, 24.9.

Synthesis of (*R*)-2-((S)-pyrrolidin-2-yl)-2-hydroxyacetic acid (2*R*,2´*S*)-7 Obtained from *tert*-butyl (*S*)-2-((*R*)-cyano(hydroxy)methyl)pyrrolidine-1-carboxylate (2*R*,2´*S*)-**22** (88 mg, 0.39 mmol), according to Method B. The residue was crystallized from ethanol, providing the desired compound (2*R*,2´*S*)-**7** in 39% yield. R_t (LC-MS) = 0.544 min. LC-MS (ESI): *m/z* calcd. for $C_6H_{12}NO_3^+$ $[M + H]^+ = 146.08$, found 146.1. ^{1}H NMR (600 MHz, D_2O) δ 4.20 (d, $J = 5.1$ Hz, 1H), 3.84 (ddd, $J = 9.2$, 7.5, 5.1 Hz, 1H), 3.43–3.31 (m, 2H), 2.27–2.18 (m, 1H), 2.17–2.09 (m, 1H), 2.09–2.01 (m, 1H), 1.97–1.87 (m, 1H). ^{13}C NMR (151 MHz, D_2O) δ 179.9, 73.4, 65.1, 48.6, 29.5, 26.3.

Synthesis of (*R*)-2-((*R*)-pyrrolidin-2-yl)-2-hydroxyacetic acid (2*R*,2´*R*)-7 Obtained from *tert*-butyl (*R*)-2-((*R*)-cyano(hydroxy)methyl)pyrrolidine-1-carboxylate (2*R*,2´*R*)-**22** (104 mg, 0.46 mmol), according to Method B. The residue

was crystallized in ethanol, providing the desired compound (2*R*,2´*R*)-**7** in 55% yield. R_t (chiral HPLC) = 9.08 min. LC-MS, ^{1}H NMR and ^{13}C NMR data as for (2*S*,2´*S*)-**7**, confirming (*R,R*) configuration of (2*R*,2´*R*)-**7**.

Synthesis of (*S*)-2-((*R*)-pyrrolidin-2-yl)-2-hydroxyacetic acid (2*S*,2´*R*)-7 Obtained from *tert*-butyl (*R*)-2-((*S*)-cyano(hydroxy)methyl)pyrrolidine-1-carboxylate (2*S*,2´*R*)-**22** (112 mg, 0.50 mmol), according to Method B. The residue was crystallized in ethanol, providing the desired compound (2*S*,2´*R*)-**7** in 41% yield. LC-MS, ^{1}H NMR and ^{13}C NMR data as for (2*R*,2´*S*)-**7**, confirming (*S,R*) configuration of (2*S*,2´*R*)-**7**.

Synthesis of (*rac*) tert-butyl 2-(cyano(hydroxy)methyl)piperidine-1-carboxylate (*rac*)$^{\#1}$-23 and of (*rac*)$^{\#2}$-23 Obtained from *tert*-butyl (*rac*)-2-formylpiperidine-1-carboxylate (*rac*)-**20** (1.00 g, 4.69 mmol), according to Method A. Purification by silica gel flash column chromatography (gradient from DCM to DCM/EtOAc 9:1) allowed separation of the two diastereoisomers (*rac*)$^{\#1}$-**23** and (*rac*)$^{\#2}$-**23**. The racemic mixture of diastereoisomer (*rac*)$^{\#1}$-**23** was obtained as a white solid in 46% yield. R_f (DCM/EtOAc 9:1) = 0.39. R_t (LC-MS) = 3.921 min. LC-MS (ESI): *m/z* calcd. for $C_8H_{13}N_2O_3$ [M-*t*Bu + H]$^+$ = 185.09, found 185.1. ^{1}H NMR (400 MHz, $CDCl_3$) δ 4.65 (d, J = 10.0 Hz, 1H), 4.46 (ddd, J = 9.6, 5.6, 3.0 Hz, 1H), 4.03 (bs, 1H), 3.90 (m, 1H), 2.90 (m, 1H), 2.03–1.94 (m, 1H), 1.82–1.63 (m, 3H), 1.54–1.48 (m, 2H), 1.47 (s, 9H). ^{13}C NMR (151 MHz, $CDCl_3$) δ 157.7, 119.3, 81.4, 61.7, 54.5, 40.9, 28.4, 24.8, 24.6, 19.5. The racemic mixture of diastereoisomer (*rac*)$^{\#2}$-**23** was obtained as a white solid in 40% yield. R_f (DCM/EtOAc 9:1) = 0.29. LC-MS (ESI): *m/z* calcd. for $C_8H_{13}N_2O_3$ [M-*t*Bu + H]$^+$ = 185.09, found 185.1. ^{1}H NMR (400 MHz, $CDCl_3$) δ 5.29 (bs, 1H), 4.61 (d, J = 5.7 Hz, 1H), 4.37 (q, J = 5.7 Hz, 1H), 4.06–3.87 (m, 1H), 3.22–2.97 (m, 1H), 2.00–1.81 (m, 1H), 1.80–1.56 (m, 5H), 1.49 (s, 9H).^{13}C NMR (151 MHz, $CDCl_3$) δ 155.8, 119.4, 81.3, 61.7, 53.6, 40.8, 28.4, 24.5, 23.8, 18.7.

Synthesis of (*rac*)-2-(pyrrolidin-2-yl)-2-hydroxyacetic acid (*rac*)$^{\#1}$-8 Obtained from *(rac)*-tert-butyl 2-(cyano(hydroxy)methyl)piperidine-1-carboxylate (*rac*)$^{\#1}$-**23** (74 mg, 0.31 mmol), according to Method B. The residue was crystallized from water/acetone, providing the desired compound (*rac*)$^{\#1}$-**8** in 47% yield. R_t (LC-MS) = 0.589 min. LC-MS (ESI): *m/z* calcd. for $C_7H_{14}NO_3^+$ $[M + H]^+$ = 160.10, found 160.1. ^{1}H NMR (600 MHz, D_2O) δ 4.02 (d, J = 5.4 Hz, 1H), 3.46 (ddt, J = 12.8, 4.2, 2.0 Hz, 1H), 3.33 (ddd, J = 11.7, 5.4, 3.1 Hz, 1H), 3.03 (td, J = 12.8, 3.1 Hz, 1H), 2.03–1.89 (m, 3H), 1.72–1.54 (m, 3H). ^{13}C NMR (151 MHz, D_2O) δ 179.6, 75.4, 61.8, 47.8, 28.1, 24.7, 24.2.

Synthesis of (*rac*)-2-(pyrrolidin-2-yl)-2-hydroxyacetic acid (*rac*)$^{\#2}$-8 Obtained from *(rac)*-tert-butyl 2-(cyano(hydroxy)methyl)piperidine-1-carboxylate (*rac*)$^{\#2}$-**23** (113 mg, 0.47 mmol), according to Method B. The residue was crystallized first from ethanol, and then from methanol/water providing the desired compound (*rac*)$^{\#2}$-**8** in 24% yield. R_t (LC-MS) = 0.581 min. LC-MS (ESI): *m/z* calcd. for $C_7H_{14}NO_3^+$ $[M + H]^+$ = 160.10, found 160.1. ^{1}H NMR (600 MHz, D_2O) δ 4.22 (d, J = 3.5 Hz, 1H), 3.53–3.41 (m, 2H), 3.10 (td, J = 13.0, 3.2 Hz, 1H), 1.99–1.84 (m, 2H), 1.74–1.60 (m, 3H), 1.60–1.49 (m, 1H). ^{13}C NMR (151 MHz, D_2O) δ 179.2, 74.3, 61.9, 47.9, 25.1, 24.5, 24.2.

Synthesis of (*rac*)-tert-butyl 3-(cyano(hydroxy)methyl)azetidine-1-carboxylate (*rac*)-29 Obtained from *tert*-butyl 3-formylazetidine-1-carboxylate **26** (360 mg, 1.96 mmol), according to Method A. Purification by silica gel flash column chromatography (*n*-heptane/EtOAc 1:1) provided the desired compound (*rac*)-**29** as a white solid in 97% yield. R_f (*n*-heptane/EtOAc 1:1) = 0.24. ^{1}H NMR (600 MHz, DMSO-d_6) δ 6.66 (d, J = 6.4 Hz, 1H), 4.74 (t, J = 6.4 Hz, 1H), 3.93–3.83 (m, 2H), 3.71–3.61 (m, 2H), 2.87 (tdt, J = 8.3, 6.4, 5.4 Hz, 1H), 1.37 (s, 9H). ^{13}C NMR (151 MHz, DMSO-d_6) δ 155.4, 119.8, 78.6, 61.2, 50.7, 49.6, 32.2, 28.0.

Synthesis of 2-(azetidin-3-yl)-2-hydroxyacetic acid (*rac*)-9 Obtained from (*rac*)-*tert*-butyl 3-(cyano(hydroxy)methyl) azetidine-1-carboxylate (*rac*)-**29** (200 mg, 0.94 mmol), according to Method B. The residue was crystallized from water/methanol, providing the desired compound (*rac*)-**9** in 21% yield. R_t (LC-MS) = 0.526 min. LC-MS (ESI): *m/z* calcd. for $C_5H_{10}NO_3^+$ $[M + H]^+$ = 132.07, found 132.1. ^{1}H NMR (600 MHz, D_2O) δ 4.27–4.19 (m, 1H), 4.17–4.06 (m, 4H), 3.35–3.25 (m, 1H). ^{13}C NMR (151 MHz, D_2O) δ 181.2, 73.5, 51.1, 49.9, 38.1.

Synthesis of tert-butyl (*S*)-3-formylpyrrolidine-1-carboxylate (*S*)-27 Obtained from *tert*-butyl (*S*)-3-(hydroxymethyl) pyrrolidine-1-carboxylate (*S*)-**24** (1.00 g, 4.97 mmol), according to Method C, providing the desired compound (*S*)-**27** in 58% yield. R_f (heptane/EtOAc 1:1) = 0.37. ^{1}H NMR (600 MHz, $CDCl_3$) δ 9.69 (t, J = 1.3 Hz, 1H), 3.77–3.64 (m, 1H), 3.58–3.47 (m, 1H), 3.44–3.29 (m, 2H), 3.02 (p, J = 6.9 Hz, 1H), 2.27–2.15 (m, 1H), 2.15–2.00 (m, 1H), 1.46 (s, 9H). ^{13}C NMR (151 MHz, $CDCl_3$) δ 200.8, 154.5, 79.8, 50.3, 45.2, 45.0, 28.6, 25.8. ^{1}H- and ^{13}C-NMR in accordance with literature [47].

Synthesis of tert-butyl (*R*)-3-formylpyrrolidine-1-carboxylate (*R*)-27 Obtained from *tert*-butyl (*R*)-3-(hydroxymethyl)pyrrolidine-1-carboxylate (*S*)-**24** (1.00 g, 4.97 mmol), according to Method C, providing the desired

compound (*R*)-**27** in 95% yield. TLC, ^{1}H NMR and ^{13}C NMR data as for (*S*)-**27**.

Synthesis of tert-butyl (3*S*)-3-(cyano(hydroxy)methyl)pyrrolidine-1-carboxylate (2*S,3´*S*)-30 and (2*R**,3´*S*)-30** Obtained from *tert*-butyl (*S*)-3-formylpyrrolidine-1-carboxylate (*S*)-**27** (578 mg, 2.90 mmol), according to Method A. Purification by silica gel flash column chromatography (gradient from *n*-heptane to *n*-heptane/EtOAc 1:1) allowed separation of the two diastereoisomers (2*S**,3´*S*)-**30** and (2*R**,3´*S*)-**30**. Diastereoisomer (2*S**,3´*S*)-**30** was obtained as a white solid in 16% yield. R_f (*n*-heptane/EtOAc 1:1) = 0.41. R_t (LC-MS) = 3.616 min. LC-MS (ESI): *m*/*z* calcd. for $C_7H_{10}N_2O_3$ $[M\text{-}tBu + H]^+ = 171.08$, found 171.0. ^{1}H NMR (600 MHz, $CDCl_3$) δ 4.38 (d, $J = 8.2$ Hz, 1H), 3.59 (dd, $J = 11.5$, 7.6 Hz, 1H), 3.55–3.47 (m, 1H), 3.41–3.29 (m, 2H), 2.64 (h, $J = 7.6$ Hz, 1H), 2.14 (h, $J = 7.0$ Hz, 1H), 1.91–1.81 (m, 1H), 1.46 (s, 9H). ^{13}C NMR (151 MHz, $CDCl_3$) δ 154.8, 119.3, 80.1, 62.7, 62.4, 47.7, 47.6, 45.3, 45.0, 43.3, 42.7, 28.4, 27.4, 26.7. Diastereoisomer (2*R**,3´*S*)-**30** was obtained as a white solid in 27% yield. R_f (*n*-heptane/EtOAc 1:1) = 0.36. R_t (LC-MS) = 3.596 min. LC-MS (ESI): *m*/*z* calcd. for $C_7H_{10}N_2O_3$ $[M\text{-}tBu + H]^+ = 171.08$, found 171.0. ^{1}H NMR (400 MHz, $CDCl_3$) δ 4.49 (d, $J = 6.7$ Hz, 1H), 3.61 (dd, $J = 11.3$, 7.8 Hz, 1H), 3.53 (ddd, $J = 12.1$, 8.3, 4.3 Hz, 1H), 3.41–3.27 (m, 2H), 3.08 (bs, 1H), 2.65 (m, 1H), 2.15–2.03 (m, 1H), 2.00–1.87 (m, 1H), 1.46 (s, 9H). ^{13}C NMR (151 MHz, $CDCl_3$) δ 154.9, 119.2, 80.3, 62.6, 62.3, 47.6, 47.2, 45.6, 45.0, 43.3, 42.5, 28.6, 27.0, 26.8.

Synthesis of tert-butyl (3*R*)-3-(cyano(hydroxy)methyl)pyrrolidine-1-carboxylate (2*R,3´*R*)-30 and (2*S**,3´*R*)-30** Obtained from *tert*-butyl (*R*)-3-formylpyrrolidine-1-carboxylate (*R*)-**27** (944 mg, 4.74 mmol), according to Method A. Purification by silica gel flash column chromatography (gradient from *n*-heptane to *n*-heptane/EtOAc 1:1) allowed separation of the two diastereoisomers (2*R**,3´*R*)-**30** and (2*S**,3´*R*)-**30**. Diastereoisomer (2*R**,3´*R*)-**30** was obtained as a white solid in 18% yield. TLC, LC-MS, ^{1}H NMR and ^{13}C NMR data as for (2*S**,3´*S*)-**30**. Diastereoisomer (2*S**,3´*R*)-**30** was obtained as a white solid in 37% yield. TLC, LC-MS, ^{1}H NMR and ^{13}C NMR data as for (2*R**,3´*S*)-**30**.

Synthesis of 2-hydroxy-2-((*S*)-pyrrolidin-3-yl)acetic acid (2*S,3´*S*)-10** Obtained from *tert*-butyl (*3S*)-3-(cyano(hydroxy)methyl)pyrrolidine-1-carboxylate (2*S**,3´*S*)-**30** (81 mg, 0.36 mmol), according to Method B. The residue was crystallized from water/ethanol, providing the desired compound (2*S**,3´*S*)-**10** in 23% yield. R_t (LC-MS) = 0.583 min. LC-MS (ESI): *m*/*z* calcd. for $C_6H_{12}NO_3^+$ $[M + H]^+ = 146.08$, found 146.1. HRMS (MALDI) *m*/*z* calcd. for $C_6H_{12}NO_3$ $[M + H]^+ = 146.0817$, found: 146.0812. ^{1}H NMR (600 MHz, D_2O) δ 4.09 (d, $J = 4.5$ Hz, 1H), 3.46 (ddd, $J = 11.3$, 8.2, 4.8 Hz, 1H), 3.40–3.28 (m, 2H), 3.22 (dd, $J = 11.8$, 8.2 Hz, 1H), 2.79 (pd, $J = 8.2$, 4.5 Hz, 1H), 2.28–2.20 (m, 1H), 1.99 (dq, $J = 13.1$, 8.2 Hz, 1H). ^{13}C NMR (151 MHz, D_2O) δ 182.2, 75.1, 48.8, 48.5, 43.9, 29.7.

Synthesis of 2-hydroxy-2-((*S*)-pyrrolidin-3-yl)acetic acid (2*R,3´*S*)-10** Obtained from *tert*-butyl (*3S*)-3-(cyano(hydroxy)methyl)pyrrolidine-1-carboxylate (2*R**,3´*S*)-**30** (150 mg, 0.66 mmol), according to Method B. The residue was decanted twice from water/ethanol, providing the desired compound (2*R**,3´*S*)-**10** in 21% yield. R_t (LC-MS) = 0.527 min. LC-MS (ESI): *m*/*z* calcd. for $C_6H_{12}NO_3^+$ $[M + H]^+ = 146.08$, found 146.1. ^{1}H NMR (600 MHz, D_2O) δ 4.09 (d, $J = 4.4$ Hz, 1H), 3.56–3.40 (m, 2H), 3.34–3.22 (m, 2H), 2.79 (pd, $J = 8.1$, 4.4 Hz, 1H), 2.12–2.02 (m, 1H), 1.95–1.86 (m, 1H). ^{13}C NMR (151 MHz, D_2O) δ 182.2, 74.6, 50.4, 48.6, 43.8, 27.5.

Synthesis of 2-hydroxy-2-((*R*)-pyrrolidin-3-yl)acetic acid (2*R,3´*R*)-10** Obtained from *tert*-butyl (*3R*)-3-(cyano(hydroxy)methyl)pyrrolidine-1-carboxylate (2*R**,3´*R*)-**30** (83 mg, 0.37 mmol), according to Method B. The residue was crystallized from water/ethanol, providing the desired compound (2*R**,3´*R*)-**10** in 19% yield. LC-MS, ^{1}H NMR and ^{13}C NMR data as for (2*S**,3´*S*)-**10**.

Synthesis of 2-hydroxy-2-((*R*)-pyrrolidin-3-yl)acetic acid (2*S,3´*R*)-10** Obtained from *tert*-butyl (*3R*)-3-(cyano(hydroxy)methyl)pyrrolidine-1-carboxylate (2*S**,3´*R*)-**30** (150 mg, 0.37 mmol), according to Method B. The residue was decanted twice from water/ethanol, providing the desired compound (2*S**,3´*R*)-**10** in 24% yield. LC-MS, ^{1}H NMR and ^{13}C NMR data as for (2*R**,3´*S*)-**10**.

Synthesis of tert-butyl (*S*)-3-formylpiperidine-1-carboxylate (*S*)-28 Obtained from *tert*-butyl (*S*)-3-(hydroxymethyl) piperidine-1-carboxylate (*S*)-**25** (1.00 g, 4.64 mmol), according to Method C, providing the desired compound (*S*)-**28** in 88% yield. ^{1}H NMR (400 MHz, $CDCl_3$) δ 9.70 (s, 1H), 4.00–3.86 (m, 1H), 3.71–3.59 (m, 1H), 3.32 (dd, $J = 13.6$, 8.3 Hz, 1H), 3.09 (ddd, $J = 13.0$, 9.3, 3.4 Hz, 1H), 2.42 (p, $J = 4.2$ Hz, 1H), 2.01–1.89 (m, 1H), 1.73–1.59 (m, 2H), 1.51–1.48 (m, 1H), 1.46 (s, 9H). ^{13}C NMR (151 MHz, $CDCl_3$) δ 202.7, 154.9, 80.1, 48.2, 44.3, 43.8, 28.6, 24.4, 23.9. ^{1}H-NMR in accordance with literature [48].

Synthesis of tert-butyl (*R*)-3-formylpiperidine-1-carboxylate (*R*)-28 Obtained from *tert*-butyl (*R*)-3-(hydroxymethyl) piperidine-1-carboxylate (*R*)-**25** (1.00 g, 4.64 mmol),

according to Method C, providing the desired compound (*R*)-**28** in 71% yield. ^{1}H NMR and ^{13}C NMR data as for (*S*)-**28**.

Synthesis of tert-butyl (3*S*)-3-(cyano(hydroxy)methyl)piperidine-1-carboxylate (2*S,3´*S*)-31 and (2*R**,3´*S*)-31** Obtained from *tert*-butyl (*S*)-3-formylpiperidine-1-carboxylate (*S*)-**28** (870 mg, 4.08 mmol), according to Method A. Purification by silica gel flash column chromatography (gradient from petroleum ether to petroleum ether/diethyl ether 1:1) allowed separation of the two diastereoisomers (2*S**,3´*S*)-**31** and (2*R**,3´*S*)-**31**. Diastereoisomer (2*S**,3´*S*)-**31** was obtained as a white solid in 13% yield. R_f (petroleum ether/diethyl ether 1:1) = 0.35. R_t (LC-MS) = 3.829 min. LC-MS (ESI): *m/z* calcd. for $C_8H_{13}N_2O_3$ $[M\text{-}tBu+H]^+ = 185.09$, found 185.1. ^{1}H NMR (600 MHz, $CDCl_3$) δ 5.11–4.86 (m, 1H), 4.32–4.20 (m, 1H), 4.03–3.93 (m, 1H), 3.86–3.68 (m, 1H), 2.98–2.85 (m, 1H), 2.85–2.72 (m, 1H), 2.02–1.79 (m, 2H), 1.71–1.58 (m, 1H), 1.49–1.35 (m, 11H). ^{13}C NMR (151 MHz, $CDCl_3$) δ 155.3, 119.1, 80.5, 63.1, 45.4, 44.9, 40.2, 28.4, 26.2, 23.9. Diastereoisomer (2*R**,3´*S*)-**31** was obtained as a white solid in 15% yield. R_f (petroleum ether/diethyl ether 1:1) = 0.28. R_t (LC-MS) = 3.836 min. LC-MS (ESI): *m/z* calcd. for $C_8H_{13}N_2O_3$ $[M\text{-}t\text{Bu} + H]^+ = 185.09$, found 185.1. ^{1}H NMR (400 MHz, $CDCl_3$) δ 4.45 (d, $J = 5.5$ Hz, 1H), 4.14–3.99 (m, 1H), 3.94–3.80 (m, 1H), 3.00–2.82 (m, 2H), 1.99–1.88 (m, 2H), 1.80–1.71 (m, 1H), 1.54–1.48 (m, 2H), 1.47 (s, 9H). ^{13}C NMR (151 MHz, $CDCl_3$) δ 155.1, 118.7, 80.3, 63.4, 45.3, 44.5, 40.2, 28.6, 25.5, 24.1.

Synthesis of tert-butyl (3*R*)-3-(cyano(hydroxy)methyl)piperidine-1-carboxylate (2*R,3´*R*)-31 and (2*S**,3´*R*)-31** Obtained from *tert*-butyl (*R*)-3-formylpiperidine-1-carboxylate (*R*)-**28** (705 mg, 3.31 mmol), according to Method A. Purification by silica gel flash column chromatography (gradient from petroleum ether to petroleum ether/diethyl ether 1:1) allowed separation of the two diastereoisomers (2*R**,3´*R*)-**31** and (2*S**,3´*R*)-**31**. Diastereoisomer (2*R**,3´*R*)-**31** was obtained as a white solid in 18% yield. TLC, LC-MS, ^{1}H NMR and ^{13}C NMR data as for (2*S**,3´*S*)-**31**. Diastereoisomer (2*S**,3´*R*)-**31** was obtained as a white solid in 32% yield. TLC, LC-MS, ^{1}H NMR and ^{13}C NMR data as for (2*R**,3´*S*)-**31**.

Synthesis of 2-hydroxy-2-((*S*)-piperidin-3-yl)acetic acid (2*S,3´*S*)-11** Obtained from *tert*-butyl (3*S*)-3-(cyano(hydroxy)methyl)piperidine-1-carboxylate (2*S**,3´*S*)-**31** (46 mg, 0.19 mmol), according to Method B. The residue was crystallized from water/ethanol, providing the desired compound (2*S**,3´*S*)-**11** in 43% yield. R_t (LC-MS) = 0.544 min. LC-MS (ESI): *m/z* calcd. for $C_7H_{14}NO_3^+$ $[M + H]^+ = 160.10$, found 160.1. ^{1}H NMR (400 MHz, D_2O) δ 3.99 (d, $J = 4.0$ Hz, 1H), 3.47–3.36 (m, 1H), 3.33–3.25 (m, 1H), 2.99–2.88 (m, 2H), 2.18 (tt, $J = 11.8$, 4.0 Hz, 1H), 2.10–1.97 (m, 1H), 1.97–1.86 (m, 1H), 1.86–1.70 (m, 1H), 1.53 (qd, $J = 12.6$, 3.9 Hz, 1H). ^{13}C NMR (151 MHz, D_2O) δ 179.4, 74.5, 45.4, 44.7, 38.0, 25.5, 22.3. ^{1}H- and ^{13}C-NMR in accordance with literature [49].

Synthesis of 2-hydroxy-2-((*S*)-piperidin-3-yl)acetic acid (2*R,3´*S*)-11** Obtained from *tert*-butyl (3*S*)-3-(cyano(hydroxy)methyl)piperidine-1-carboxylate (2*R**,3´*S*)-**31** (80 mg, 0.33 mmol), according to Method B. The residue was crystallized from water/ethanol, providing the desired compound (2*R**,3´*S*)-**11** in 47% yield. R_t (LC-MS) = 0.532 min. LC-MS (ESI): *m/z* calcd. for $C_7H_{14}NO_3^+$ $[M + H]^+ = 160.10$, found 160.1. ^{1}H NMR (600 MHz, D_2O) δ 3.99 (d, $J = 3.7$ Hz, 1H), 3.49–3.44 (m, 1H), 3.44–3.37 (m, 1H), 2.97–2.88 (m, 2H), 2.21 (tq, $J = 11.2$, 3.7 Hz, 1H), 2.06–1.98 (m, 1H), 1.79–1.66 (m, 2H), 1.50 (qd, $J = 12.9$, 4.0 Hz, 1H). ^{13}C NMR (151 MHz, D_2O) δ 181.7, 76.0, 49.3, 46.9, 40.0, 25.0, 24.5. ^{1}H- and ^{13}C-NMR in accordance with literature [49].

Synthesis of 2-hydroxy-2-((*R*)-piperidin-3-yl)acetic acid (2*R,3´R)-11** Obtained from *tert*-butyl (3*R*)-3-(cyano(hydroxy)methyl)piperidine-1-carboxylate (2*R**,3´*R*)-**31** (97 mg, 0.40 mmol), according to Method B. The residue was crystallized from water/ethanol, providing the desired compound (2*R**,3´*R*)-**11** in 30% yield. LC-MS, ^{1}H NMR and ^{13}C NMR data as for (2*S**,3´*S*)-**11**.

Synthesis of 2-hydroxy-2-((*R*)-piperidin-3-yl)acetic acid (2*S,3´*R*)-11** Obtained from *tert*-butyl (3*R*)-3-(cyano(hydroxy)methyl)piperidine-1-carboxylate (2*S**,3´*R*)-**31** (120 mg, 0.40 mmol), according to Method B. The residue was crystallized from water/ethanol, providing the desired compound (2*S**,3´*R*)-**11** in 17% yield. LC-MS, ^{1}H NMR and ^{13}C NMR data as for (2*R**,3´*S*)-**11**.

Synthesis of (*S*)-2-((*S*)-1-benzylazetidin-2-yl)-2-hydroxyacetic acid (2*S*,2´*S*)-6a Obtained from (*S*)-2-((*S*)-azetidin-2-yl)-2-hydroxyacetic acid (2*S*,2´*S*)-**6** (30 mg, 0.23 mmol) and benzaldehyde according to Method D. The crude was purified by preparative HPLC followed by ion exchange chromatography, and crystallized from water/ethanol, providing the desired compound in 49% yield. R_t (LC-MS) = 1.488 min. LC-MS (ESI): *m/z* calcd. for $C_{12}H_{16}NO_3^+$ $[M + H]^+ = 222.11$, found 222.2. R_t (HPLC) = 6.31 min. ^{1}H NMR (600 MHz, MeOD) δ 7.57–7.50 (m, 2H), 7.50–7.43 (m, 3H), 4.74 (td, $J = 8.8$, 3.8 Hz, 1H), 4.41 (d, $J = 12.9$ Hz, 1H), 4.34 (d, $J = 12.9$ Hz, 1H), 4.05–3.96 (m, 1H), 3.96–3.88 (m, 1H), 3.67–3.54 (m, 1H), 2.47 (dq, $J = 11.8$, 9.3 Hz, 1H), 2.35–2.22 (m, 1H). ^{13}C NMR (151 MHz, MeOD) δ 174.8, 131.4, 131.3, 131.0, 130.4, 71.4, 70.3, 58.8, 52.3, 18.0.

Synthesis of (*S*)-2-((*S*)-1-([1,1'-biphenyl]-3-ylmethyl)azetidin-2-yl)-2-hydroxyacetic acid (2*S*,2´*S*)-6b Obtained from (*S*)-2-((*S*)-azetidin-2-yl)-2-hydroxyacetic acid (2*S*,2´*S*)-**6** (40 mg, 0.31 mmol), and [1,1'-biphenyl]-3-carbaldehyde, according to Method D. The crude was purified by preparative preparative HPLC followed by ion exchange chromatography, and crystallized from water/ethanol providing the desired compound in 32% yield. R_t (LC-MS) = 3.120 min. LC-MS (ESI): *m/z* calcd. for $C_{18}H_{20}NO_3^+$ $[M + H]^+ = 298.14$, found 298.2. R_t (HPLC) = 10.37 min. ^{1}H NMR (600 MHz, MeOD) δ 7.79 (t, $J = 1.6$ Hz, 1H), 7.71 (dt, $J = 7.6$, 1.6 Hz, 1H), 7.68–7.64 (m, 2H), 7.53 (t, $J = 7.6$ Hz, 1H), 7.49 (dt, $J = 7.6$, 1.6 Hz, 1H), 7.45 (t, $J = 7.7$ Hz, 2H), 7.39–7.34 (m, 1H), 4.74 (td, $J = 8.7$, 3.8 Hz, 1H), 4.46 (d, $J = 12.9$ Hz, 1H), 4.39 (d, $J = 12.9$ Hz, 1H), 4.02–3.95 (m, 1H), 3.93 (td, $J = 9.7$, 4.6 Hz, 1H), 3.75–3.67 (m, 1H), 2.54–2.42 (m, 1H), 2.34–2.24 (m, 1H). ^{13}C NMR (151 MHz, MeOD) δ 175.0, 143.7, 141.5, 132.2, 130.9, 130.03, 129.99, 129.9, 129.4, 128.9, 128.2, 71.5, 70.5, 58.9, 52.4, 18.0.

Synthesis of (*S*)-2-((*S*)-1-([1,1'-biphenyl]-4-ylmethyl)azetidin-2-yl)-2-hydroxyacetic acid (2*S*,2´*S*)-6c Obtained from (*S*)-2-((*S*)-azetidin-2-yl)-2-hydroxyacetic acid (2*S*,2´*S*)-**6** (40 mg, 0.31 mmol) and [1,1'-biphenyl]-4-carbaldehyde [according to Method D. The crude was purified by preparative HPLC followed by ion exchange chromatography, providing the desired compound in 39% yield. R_t (LC-MS) = 3.076 min. LC-MS (ESI): *m/z* calcd. for $C_{18}H_{20}NO_3^+$ $[M + H]^+ = 298.14$, found 298.1. R_t (HPLC) = 10.41 min. ^{1}H NMR (600 MHz, DMSO-d_6) δ 7.68–7.64 (m, 2H), 7.62 (d, $J = 8.2$ Hz, 2H), 7.48–7.44 (m, 2H), 7.42 (d, $J = 8.2$ Hz, 2H), 7.37–7.33 (m, 1H), 4.07 (bs, 2H, exchanges with D_2O), 4.03 (d, $J = 13.2$ Hz, 1H), 3.78 (td, $J = 8.2$, 3.8 Hz, 1H), 3.68 (d, $J = 3.8$ Hz, 1H), 3.67 (d, $J = 13.2$ Hz, 1H), 3.30 (td, $J = 8.2$, 3.2 Hz, 1H), 3.05 (q, $J = 8.2$ Hz, 1H), 2.14–2.05 (m, 1H), 1.90 (dtd, $J = 10.9$, 8.2, 3.2 Hz, 1H). ^{13}C NMR (151 MHz, DMSO-d_6) δ 173.0, 139.8, 139.2, 135.8, 129.4, 128.9, 127.4, 126.6, 126.5, 71.1, 68.2, 59.5, 50.5, 18.0.

Synthesis of (*S*)-2-((*S*)-1-(4-(benzyloxy)benzyl)azetidin-2-yl)-2-hydroxyacetic acid (2*S*,2´*S*)-6d Obtained from (*S*)-2-((*S*)-azetidin-2-yl)-2-hydroxyacetic acid (2*S*,2´*S*)-**6** (40 mg, 0.31 mmol) and 4-(benzyloxy)benzaldehyde according to Method D. The crude was purified by preparative HPLC followed by ion exchange chromatography, providing the desired compound in 57% yield. R_t (LC-MS) = 3.126 min. LC-MS (ESI): *m/z* calcd. for $C_{19}H_{22}NO_4^+$ $[M + H]^+ = 328.15$, found 328.2. R_t (HPLC) = 10.73 min. ^{1}H NMR (600 MHz, DMSO-d_6) δ 7.44 (d, $J = 7.1$ Hz, 2H), 7.38 (t, $J = 7.5$ Hz, 2H), 7.35–7.29 (m, 1H), 7.28 (d, $J = 8.5$ Hz, 2H), 6.97 (d, $J = 8.5$ Hz, 2H), 5.08 (s, 2H), 4.44 (bs, 2H, exchanges with D_2O), 3.96 (d, $J = 12.8$ Hz, 1H), 3.86 (td, $J = 8.4$, 3.6 Hz, 1H), 3.66 (d, $J = 12.8$ Hz, 1H), 3.55 (d, $J = 3.6$ Hz, 1H), 3.36–3.26 (m, 1H), 3.10 (q, $J = 8.4$ Hz, 1H), 2.13–2.03 (m, 1H), 1.87 (dtd, $J = 11.4$, 8.4, 3.4 Hz, 1H). ^{13}C NMR (151 MHz, DMSO-d_6) δ 172.8, 157.9, 137.1, 130.4, 128.4, 127.8, 127.7, 114.6, 70.7, 69.2, 68.4, 58.6, 50.1, 17.5.

Synthesis of (*S*)-2-hydroxy-2-((*S*)-1-(4-hydroxybenzyl)azetidin-2-yl)acetic acid (2*S*,2´*S*)-6e Obtained from (*S*)-2-((*S*)-azetidin-2-yl)-2-hydroxyacetic acid (2*S*,2´*S*)-**6** (40 mg, 0.31 mmol) and 4-hydroxybenzaldehyde, according to Method D. The crude was purified by preparative HPLC (isocratic 20% B) followed by ion exchange chromatography and crystallization from ethanol/water, providing the desired compound in 31% yield. R_t (LC-MS) = 0.812 min. LC-MS (ESI): *m/z* calcd. for $C_{12}H_{16}NO_4^+$ $[M + H]^+ = 238.11$, found 238.2. R_t (HPLC) = 5.25 min. ^{1}H NMR (600 MHz, D_2O) δ 7.43 (d, $J = 8.5$ Hz, 2H), 6.99 (d, $J = 8.5$ Hz, 2H), 4.82 (td, $J = 9.0$, 3.7 Hz, 1H), 4.38 (d, $J = 13.1$ Hz, 1H), 4.33 (d, $J = 13.1$ Hz, 1H), 4.05 (q, $J = 9.8$ Hz, 1H), 3.99 (td, $J = 9.8$, 4.3 Hz, 1H), 3.71–3.60 (m, 1H), 2.54–2.44 (m, 1H), 2.36–2.26 (m, 1H). ^{13}C NMR (151 MHz, D_2O) δ 178.0, 159.9, 134.8, 124.0, 119.0, 71.7, 71.6, 59.9, 53.8, 19.3.

Synthesis of (*S*)-2-((*S*)-1-(4-acetamidobenzyl)azetidin-2-yl)-2-hydroxyacetic acid (2*S*,2´*S*)-6f Obtained from (*S*)-2-((*S*)-azetidin-2-yl)-2-hydroxyacetic acid (2*S*,2´*S*)-**6** (40 mg, 0.31 mmol) and 4-acteamidobenzaldehyde, according to Method D. The crude was purified by preparative HPLC followed by ion exchange chromatography, providing the desired compound in 71% yield. R_t (LC-MS) = 1.096 min. LC-MS (ESI): *m/z* calcd. for $C_{14}H_{19}N_2O_4^+$ $[M + H]^+ = 279.13$, found 279.1. R_t (HPLC) = 5.99 min. ^{1}H NMR (600 MHz, MeOD) δ 7.66 (d, $J = 8.6$ Hz, 2H), 7.46 (d, $J = 8.6$ Hz, 2H), 4.72 (td, $J = 8.8$, 3.8 Hz, 1H), 4.36 (d, $J = 13.0$ Hz, 1H), 4.29 (d, $J = 13.0$ Hz, 1H), 4.01–3.94 (m, 1H), 3.91 (td, $J = 9.8$, 4.6 Hz, 1H), 3.68–3.59 (m, 1H), 2.52–2.42 (m, 1H), 2.32–2.24 (m, 1H), 2.13 (s, 3H). ^{13}C NMR (151 MHz, MeOD) δ 174.9, 171.8, 141.6, 132.0, 126.4, 121.4, 71.2, 70.3, 58.3, 52.1, 23.9, 17.9.

Synthesis of (*S*)-2-((*S*)-1-benzylpyrrolidin-2-yl)-2-hydroxyacetic acid (2*S*,2´*S*)-7a Obtained from (*S*)-2-hydroxy-2-((*S*)-pyrrolidin-2-yl)acetic acid (2*S*,2´*S*)-**7** (40 mg, 0.31 mmol) and benzaldehyde, according to Method D. The crude was purified by preparative HPLC (gradient from 0% to 90% B) followed by ion exchange chromatography, providing the desired compound in 89% yield. R_t (LC-MS) = 0.625 min. LC-MS (ESI): *m/z* calcd. for $C_{13}H_{18}NO_3^+$ $[M + H]^+ = 236.13$, found 236.1. R_t (HPLC) = 6.63 min. ^{1}H NMR (600 MHz, $CDCl_3$) δ 7.53–7.47 (m, 2H), 7.41–7.34 (m,

3H), 6.18 (bs, 2H), 4.37 (d, $J = 12.7$ Hz, 1H), 4.25–4.11 (m, 2H), 3.99–3.78 (m, 1H), 3.43–3.30 (m, 1H), 3.06–2.92 (m, 1H), 2.21–2.13 (m, 1H), 2.13–1.98 (m, 2H), 1.98–1.86 (m, 1H). ^{13}C NMR (151 MHz, DMSO-d_6) δ 174.1, 129.1, 128.3, 127.4, 69.8, 66.6, 57.8, 52.8, 25.2, 22.5.

Synthesis of (*S*)-2-((*S*)-1-([1,1'-biphenyl]-3-ylmethyl)pyrrolidin-2-yl)-2-hydroxyacetic acid TFA (2*S*,2´*S*)-7b Obtained from (*S*)-2-hydroxy-2-((*S*)-pyrrolidin-2-yl)acetic acid (2*S*,2´*S*)-**7** (20 mg, 0.15 mmol) and [1,1'-biphenyl]-3-carbaldehyde, according to Method D. The crude was purified by preparative HPLC providing the desired compound as a colorless oil in 42% yield. R_t (LC-MS) = 3.194 min. LC-MS (ESI): *m/z* calcd. for $C_{19}H_{22}NO_3^+$ $[M + H]^+ = 312.16$, found 312.2. R_t (HPLC) = 10.60 min. ^{1}H NMR (600 MHz, $CDCl_3$) δ 11.48 (bs, 1H), 7.75–7.73 (m, 1H), 7.71 (dt, $J = 7.9$, 1.4 Hz, 1H), 7.62–7.58 (m, 2H), 7.54 (t, $J = 7.7$ Hz, 1H), 7.48–7.43 (m, 3H), 7.41–7.36 (m, 1H), 5.35 (bs, 2H), 4.45 (d, $J = 12.9$ Hz, 1H), 4.36–4.31 (m, 1H), 4.28 (d, $J = 12.9$ Hz, 1H), 4.19 (t, $J = 7.1$ Hz, 1H), 3.76–3.66 (m, 1H), 3.19–3.09 (m, 1H), 2.23–2.02 (m, 4H). ^{13}C NMR (101 MHz, $CDCl_3$) δ 170.7, 143.2, 139.6, 130.3, 129.8, 129.8, 129.6, 129.2, 128.6, 128.3, 127.3, 68.4, 68.2, 59.7, 55.4, 24.6, 23.6.

Synthesis of (*S*)-2-((*S*)-1-([1,1'-biphenyl]-4-ylmethyl)pyrrolidin-2-yl)-2-hydroxyacetic acid (2*S*,2´*S*)-7c Obtained from (*S*)-2-hydroxy-2-((*S*)-pyrrolidin-2-yl)acetic acid (2*S*,2´*S*)-**7** (20 mg, 0.15 mmol) and [1,1'-biphenyl]-4-carbaldehyde, according to Method D. The crude was purified by preparative HPLC followed by ion exchange chromatography, and crystallized from water/ethanol, providing the desired compound in 38% yield. R_t (LC-MS) = 3.178 min. LC-MS (ESI): *m/z* calcd. for $C_{19}H_{22}NO_3^+$ $[M + H]^+ = 312.16$, found 312.1. R_t (HPLC) = 10.59 min. ^{1}H NMR (600 MHz, DMSO-d_6) δ 7.72–7.61 (m, 4H), 7.52–7.43 (m, 4H), 7.38–7.33 (m, 1H), 4.26 (d, $J = 13.2$ Hz, 1H), 3.93 (d, $J = 4.8$ Hz, 1H), 3.68 (d, $J = 13.2$ Hz, 1H), 3.41–3.22 (bs, 2H), 3.16 (dt, $J = 8.8$, 4.8 Hz, 1H), 2.99–2.93 (m, 1H), 2.53–2.51 (m, 1H), 1.90–1.69 (m, 4H). ^{13}C NMR (151 MHz, DMSO-d_6) δ 174.0, 139.8, 139.3, 136.1, 129.8, 128.9, 127.4, 126.6, 126.6, 69.8, 66.6, 57.4, 52.8, 25.4, 22.5.

Synthesis of tert-butyl (*S*)-2-(methoxy(methyl)carbamoyl) azetidine-1-carboxylate (*S*)-33 (*S*)-1-(tert-butoxycarbonyl) azetidine-2-carboxylic acid (*S*)-**32** (5.00 g, 24.9 mmol) and *N,O*-dimethylhydroxylamine hydrochloride (2.95 g, 30.3 mmol, 1.22 eq) were dissolved in DMF (50 ml) and the solution was cooled to 0 °C. Upon sequential addition of *N*-methylmorpholine (3.33 ml, 30.3 mmol, 1.22 eq), HOBt (4.09 g, 30.3 mmol, 1.22 eq), and EDC (4.70 g, 30.3 mmol, 1.22 eq), the reaction mixture was stirred at 0 °C for 2 h and then at room temperature overnight. The mixture was diluted with EtOAc (300 ml), washed with HCl 1 M, NaOH 1 M and with brine. The organic layer was dried over anhydrous sodium sulfate, filtered and the solvent was evaporated under vacuum, providing the desired product as a colorless oil that solidified upon standing, in 56% yield. R_f (DCM/EtOAc 95:5) = 0.39. R_t (LC-MS) = 3.457 min. LC-MS (ESI): *m/z* calcd. for $C_{11}H_{21}N_2O_4^+$ $[M + H]^+ = 245.15$, found 245.2. ^{1}H NMR (400 MHz, $CDCl_3$) δ 5.03 (dd, $J = 9.0$, 5.5 Hz, 1H), 4.05 (dd, $J = 9.0$, 6.3 Hz, 1H), 3.87 (ddd, $J = 9.0$, 7.9, 5.5 Hz, 1H), 3.71 (s, 3H), 3.22 (s, 3H), 2.46 (dtd, $J = 11.1$, 9.0, 6.2 Hz, 1H), 2.12 (ddt, $J = 11.1$, 9.0, 5.5 Hz, 1H), 1.43 (s, 9H). ^{1}H- and ^{13}C-NMR data in accordance with literature [50].

Synthesis of tert-butyl (*S*)-2-acetylazetidine-1-carboxylate (*S*)-34 Under inert atmosphere, intermediate (*S*)-**33** (524 mg, 2.14 mmol) was dissolved in dry THF (12 ml) and cooled to −78 °C. A solution of MeMgCl 3 M in THF (1.07 ml, 3.22 mmol, 1.5 eq) was added dropwise and the resulting solution was stirred at the same temperature for 2 h. The reaction mixture was slowly quenched with saturated NH_4Cl_{aq} (25 ml) and extracted with EtOAc (3 × 25 ml). The combined organic phase was dried over anhydrous sodium sulfate, filtered, and the solvent was evaporated under vacuum. The crude was purified by silica gel flash column chromatography (gradient from petroleum ether/AcOEt 9:1 to 8:2), providing the desired product as a white solid in 92% yield. R_f (petroleum ether/AcOEt 9:1) = 0.18. R_t (LC-MS) = 3.655 min. LC-MS (ESI): *m/z* calcd. for $C_6H_{10}NO_3^+$ $[M + H\text{-}t\text{Bu}]^+ = 144.07$, found 144.1. ^{1}H NMR (400 MHz, $CDCl_3$) δ 4.59 (dd, $J = 9.7$, 6.1 Hz, 1H), 4.00–3.82 (m, 2H), 2.45 (tdd, $J = 11.6$, 9.7, 5.9 Hz, 1H), 2.25 (s, 3H), 2.12 (ddt, $J = 11.6$, 8.8, 6.4 Hz, 1H), 1.43 (s, 9H). ^{13}C NMR (151 MHz, $CDCl_3$) δ 207.7, 156.1, 80.4, 67.0, 47.0, 28.4, 26.1, 19.8. ^{1}H- and ^{13}C-NMR data in accordance with literature [50].

Synthesis of tert-butyl (2*S*)-2-(1-cyano-1-hydroxyethyl)azetidine-1-carboxylate (2*S,2´*S*)-35 and (2*R**,2´*S*)-35** Obtained from intermediate (*S*)-**34** (380 mg, 1.91 mmol) according to Method A. Purification by silica gel flash column chromatography (gradient from DCM to DCM/EtOAc 95:5) allowed separation of the two diastereoisomers (2*S**,2´*S*)-**35** and (2*R**,2´*S*)-**35**. Diastereoisomer (2*S**,2´*S*)-**35** was obtained as a white solid in 83% yield. R_f (DCM/EtOAc 95:5) = 0.82. ^{1}H NMR (600 MHz, $CDCl_3$) δ 6.77 (s, 1H), 4.25 (dd, $J = 8.5$, 6.7 Hz, 1H), 3.96–3.86 (m, 2H), 2.35–2.27 (m, 1H), 2.20–2.10 (m, 1H), 1.47 (s, 9H), 1.42 (s, 3H). ^{13}C NMR (151 MHz, $CDCl_3$) δ 158.2, 120.1, 82.1, 73.2, 68.8, 46.9, 28.4, 22.4, 19.1. Diastereoisomer (2*R**,2´*S*)-**35** was obtained as a white solid in 11% yield. R_f (DCM/EtOAc 95:5) = 0.43. ^{1}H NMR (600 MHz, $CDCl_3$) δ

5.29 (bs, 1H), 4.54 (t, $J = 7.8$ Hz, 1H), 3.90 (td, $J = 8.9$, 6.6 Hz, 1H), 3.80 (td, $J = 8.9$, 5.3 Hz, 1H), 2.43–2.35 (m, 1H), 2.17–2.06 (m, 1H), 1.62 (s, 3H), 1.45 (s, 9H). ^{13}C NMR (151 MHz, $CDCl_3$) δ 157.8, 120.1, 81.9, 70.4, 67.5, 47.0, 28.3, 22.2, 18.5.

Synthesis of 2-((*S*)-azetidin-2-yl)-2-hydroxypropanoic acid (2*S,2′*S*)-12** Obtained from intermediate (2*S**,2′*S*)-**35** (230 mg, 1.02 mmol) according to Method B, providing the desired compound (2*S**,2′*S*)-**12** in 53% yield. R_t (LC-MS) = 0.558 min. LC-MS (ESI): *m/z* calcd. for $C_6H_{12}NO_3^+$ $[M + H]^+ = 146.08$, found 146.1. ^{1}H NMR (600 MHz, D_2O) δ 4.75 (t, $J = 8.9$ Hz, 1H), 4.14–4.06 (m, 1H), 3.86 (td, $J = 10.0$, 5.2 Hz, 1H), 2.55–2.45 (m, 1H), 2.44–2.36 (m, 1H), 1.37 (s, 3H). ^{13}C NMR (151 MHz, D_2O) δ 180.8, 77.0, 68.6, 45.6, 24.4, 22.5.

Synthesis of 2-((*S*)-azetidin-2-yl)-2-hydroxypropanoic acid (2*R,2′*S*)-12** Obtained from intermediate (2*R**,2′*S*)-**35** (36 mg, 0.16 mmol) according to Method B. The residue was crystallized from water/ethanol, providing the desired compound (2*R**,2′*S*)-**12** in 57% yield. R_t (LC-MS) = 0.562 min. LC-MS (ESI): *m/z* calcd. for $C_6H_{12}NO_3^+$ $[M + H]^+ = 146.08$, found 146.1. ^{1}H NMR (600 MHz, D_2O) δ 4.84–4.81 (m, 1H), 4.17 (dt, $J = 10.3$, 9.2 Hz, 1H), 3.90 (td, $J = 10.3$, 5.3 Hz, 1H), 2.69–2.55 (m, 2H), 1.37 (s, 3H). ^{13}C NMR (151 MHz, D_2O) δ 181.4, 77.0, 67.5, 45.6, 23.7, 22.8.

Synthesis of methyl (*S*)-2-((*S*)-azetidin-2-yl)-2-hydroxyacetate (2*S*,2′*S*)-36 Obtained from (2*S*,2′*S*)-**6** (110 mg, 0.84 mmol) according to Method E as an off-white solid in 85% yield. R_t (LC-MS) = 0.507 min. LC-MS (ESI): *m/z* calcd. for $C_6H_{12}NO_3^+$ $[M + H]^+ = 146.08$, found 146.1. ^{1}H NMR (600 MHz, MeOD) δ 4.77 (td, $J = 8.4$, 4.2 Hz, 1H), 4.55 (d, $J = 4.2$ Hz, 1H), 4.03 (q, $J = 9.3$ Hz, 1H), 3.92–3.84 (m, 1H), 3.77 (s, 3H), 2.67–2.55 (m, 1H), 2.51–2.41 (m, 1H). ^{13}C NMR (151 MHz, MeOD) δ 171.8, 69.9, 62.0, 53.1, 44.8, 20.5.

Synthesis of methyl (*S*)-2-hydroxy-2-((*S*)-pyrrolidin-2-yl) acetate (2*S*,2′*S*)-37 Obtained from (2*S*,2′*S*)-**7** (100 mg, 0.69 mmol) according to Method E as an off-white solid in 92% yield. R_t (LC-MS) = 0.535 min. LC-MS (ESI): *m/z* calcd. for $C_7H_{14}NO_3^+$ $[M + H]^+ = 160.10$, found 160.1.^{1}H NMR (600 MHz, MeOD) δ 4.54 (d, $J = 4.2$ Hz, 1H), 3.94 (td, $J = 7.9$, 4.2 Hz, 1H), 3.80 (s, 3H), 3.31–3.27 (m, 2H), 2.14–1.91 (m, 4H). ^{13}C NMR (151 MHz, MeOD) δ 172.7, 69.7, 62.2, 53.1, 47.5, 25.4, 24.9.

Synthesis of methyl (*R*)-2-hydroxy-2-((*S*)-pyrrolidin-2-yl) acetate (2*R*,2′*S*)-37 Obtained from (2*R*,2′*S*)-**7** (154 mg, 1.06 mmol) according to Method E as an off-white solid in 74% yield. R_t (LC-MS) = 0.650 min. LC-MS (ESI): *m/z* calcd. for $C_7H_{14}NO_3^+$ $[M + H]^+ = 160.09$, found 160.1. ^{1}H NMR (600 MHz, MeOD) δ 4.37 (d, $J = 4.4$ Hz, 1H), 3.88 (td, $J = 8.2$, 4.4 Hz, 1H), 3.82 (s, 3H), 3.30–3.28 (m, 2H), 2.26–2.18 (m, 1H), 2.15–2.08 (m, 1H), 2.07–1.96 (m, 2H). ^{13}C NMR (151 MHz, MeOD) δ 173.0, 70.4, 62.6, 53.1, 47.2, 28.1, 24.9.

Synthesis of methyl (*R*)-2-hydroxy-2-((*R*)-pyrrolidin-2-yl) acetate (2*R*,2′*R*)-37 Obtained from (2*R*,2′*R*)-**7** (146 mg, 0.90 mmol) according to Method E as an off-white solid in 90% yield. LC-MS, ^{1}H NMR and ^{13}C NMR data as for (2*S*,2′*S*)-**37**.

Synthesis of methyl (*S*)-2-hydroxy-2-((*R*)-pyrrolidin-2-yl) acetate (2*S*,2′*R*)-37 Obtained from (2*S*,2′*R*)-**7** (145 mg, 1.03 mmol) according to Method E as an off-white solid in 75% yield. LC-MS, ^{1}H NMR and ^{13}C NMR data as for (2*R*,2′*S*)-**37**.

Synthesis of methyl (*S*)-2-hydroxy-2-((*S*)-1-((E)-4,4,4-tris(4-methoxyphenyl)but-2-en-1-yl)azetidin-2-yl)acetate (2*S*,2′*S*)-38g Obtained from (2*S*,2′*S*)-**36** (50 mg, 0.31 mmol) according to Method F as an off-white solid in 37% yield, after purification with preparative HPLC (isocratic 40% B). R_t (LC-MS) = 3.888 min. LC-MS (ESI): *m/z* calcd. for $C_{31}H_{36}NO_6^+$ $[M + H]^+ = 518.25$, found 518.3. ^{1}H NMR (600 MHz, MeOD) δ 7.14 (d, $J = 15.3$ Hz, 1H), 6.97 (d, $J = 8.8$ Hz, 6H), 6.86–6.82 (m, 6H), 5.25 (dt, $J = 15.3$, 7.2 Hz, 1H), 4.78 (td, $J = 8.6$, 3.3 Hz, 2H), 4.37–4.29 (m, 1H), 4.08–3.99 (m, 1H), 3.99–3.94 (m, 1H), 3.94–3.87 (m, 2H), 3.78 (s, 9H), 3.74 (s, 3H), 2.62–2.52 (m, 1H), 2.40–2.30 (m, 1H). ^{13}C NMR (151 MHz, MeOD) δ 171.2, 159.7, 151.0, 138.7, 132.1, 120.0, 114.2, 69.2, 69.0, 60.2, 57.5, 55.7, 53.2, 52.1, 17.1.

Synthesis of methyl (*S*)-2-hydroxy-2-((*S*)-1-((E)-4,4,4-tris(4-methoxyphenyl)but-2-en-1-yl)pyrrolidin-2-yl)acetate (2*S*,2′*S*)-39g Obtained from (2*S*,2′*S*)-**37** (80 mg, 0.50 mmol) according to Method F as an off-white solid in 19% yield. R_t (LC-MS) = 3.984 min. LC-MS (ESI): *m/z* calcd. for $C_{32}H_{38}NO_6^+$ $[M + H]^+ = 532.27$, found 532.2. ^{1}H NMR (600 MHz, MeOD) δ 7.14 (d, $J = 15.4$ Hz, 1H), 6.99 (d, $J = 8.9$ Hz, 6H), 6.84 (d, $J = 8.9$ Hz, 6H), 5.38 (dt, $J = 15.0$, 7.3 Hz, 1H), 4.57 (d, $J = 3.0$ Hz, 1H), 4.16 – 4.07 (m, 1H), 3.97–3.87 (m, 2H), 3.77 (s, 9H), 3.73 (s, 3H), 3.55–3.48 (m, 1H), 3.22–3.14 (m, 1H), 2.11–1.97 (m, 4H). ^{13}C NMR (151 MHz, MeOD) δ 172.2, 159.7, 150.7, 138.7, 132.1, 120.8, 114.2, 68.7, 68.4, 60.2, 57.0, 56.0, 55.7, 53.1, 25.0, 23.4.

Synthesis of methyl (*R*)-2-hydroxy-2-((*S*)-1-((E)-4,4,4-tris(4-methoxyphenyl)but-2-en-1-yl)pyrrolidin-2-yl)acetate (2*R*,2´*S*)-39g Obtained from (2*R*,2´*S*)-**37** (51 mg, 0.32 mmol) according to Method F as an off-white solid in 25% yield. R_t (LC-MS) = 4.137 min. LC-MS (ESI): *m/z* calcd. for $C_{32}H_{38}NO_6^+$ $[M + H]^+ = 532.27$, found 532.3. ^{1}H NMR (600 MHz, MeOD) δ 7.05 (d, $J = 15.4$ Hz, 1H), 6.97 (d, $J = 8.9$ Hz, 6H), 6.85 (d, $J = 8.9$ Hz, 6H), 5.37 (ddd, $J = 15.4$, 8.3, 6.4 Hz, 1H), 4.31 (d, $J = 6.5$ Hz, 1H), 4.15–4.06 (m, 1H), 3.89–3.81 (m, 2H), 3.78 (s, 9H), 3.77 (s, 3H), 3.47–3.40 (m, 1H), 3.26–3.15 (m, 1H), 2.34–2.24 (m, 1H), 2.13–2.05 (m, 1H), 2.04–1.94 (m, 2H). ^{13}C NMR (151 MHz, MeOD) δ 172.8, 159.8, 150.6, 138.8, 132.1, 120.9, 114.2, 71.3, 69.2, 60.3, 59.1, 55.7, 55.2, 53.2, 28.7, 23.7.

Synthesis of methyl (*R*)-2-hydroxy-2-((*R*)-1-((E)-4,4,4-tris(4-methoxyphenyl)but-2-en-1-yl)pyrrolidin-2-yl)acetate (2*R*,2´*R*)-39g Obtained from (2*R*,2´*R*)-**37** (41 mg, 0.26 mmol) according to Method F as an off-white solid in 14% yield. LC-MS, ^{1}H NMR and ^{13}C NMR data as for (2*S*,2´*S*)-**39g**.

Synthesis of methyl (*S*)-2-hydroxy-2-((*R*)-1-((E)-4,4,4-tris(4-methoxyphenyl)but-2-en-1-yl)pyrrolidin-2-yl)acetate (2*S*,2´*R*)-39g Obtained from (2*S*,2´*R*)-**37** (49 mg, 0.31 mmol) according to Method F as an off-white solid in 22% yield. LC-MS, ^{1}H NMR and ^{13}C NMR data as for (2*R*,2´*S*)-**39g**.

Synthesis of (*S*)-2-hydroxy-2-((*S*)-1-((E)-4,4,4-tris(4-methoxyphenyl)but-2-en-1-yl)azetidin-2-yl)acetic acid (2*S*,2´*S*)-6g Obtained from (2*S*,2´*S*)-**38g** (35 mg, 0.07 mmol) according to Method G as an off-white solid in 74% yield. R_t (LC-MS) = 3.755 min. LC-MS (ESI): *m/z* calcd. for $C_{30}H_{34}NO_6^+$ $[M + H]^+ = 504.24$, found 504.2. R_t (HPLC) = 13.30 min. ^{1}H NMR (600 MHz, MeOD) δ 7.14 (d, $J = 15.1$ Hz, 1H), 6.97 (d, $J = 8.8$ Hz, 7H), 6.84 (d, $J = 8.8$ Hz, 7H), 5.26 (dt, $J = 15.1$, 7.4 Hz, 1H), 4.83–4.76 (m, 1H), 4.27 (d, $J = 3.4$ Hz, 1H), 4.04 (dd, $J = 13.0$, 7.4 Hz, 1H), 4.00–3.93 (m, 1H), 3.93–3.87 (m, 2H), 3.78 (s, 9H), 2.62–2.52 (m, 1H), 2.39–2.30 (m, 1H). ^{13}C NMR (151 MHz, MeOD) δ 172.5, 159.8, 150.9, 138.7, 132.1, 120.1, 114.2, 69.8, 69.1, 60.2, 57.5, 55.7, 51.9, 17.2.

Synthesis of (*S*)-2-hydroxy-2-((*S*)-1-((E)-4,4,4-tris(4-methoxyphenyl)but-2-en-1-yl)pyrrolidin-2-yl)acetic acid (2*S*,2´*S*)-7g Obtained from (2*S*,2´*S*)-**39g** (20 mg, 0.04 mmol) according to Method G as a white solid in 70% yield. R_t (LC-MS) = 3.874 min. LC-MS (ESI): *m/z* calcd. for $C_{31}H_{36}NO_6^+$ $[M + H]^+ = 518.25$, found 518.2. R_t (HPLC) = 13.45 min. ^{1}H NMR (600 MHz, MeOD) δ 7.13 (d, $J = 15.4$ Hz, 1H), 6.99 (d, $J = 8.9$ Hz, 6H), 6.84 (d, $J = 8.9$ Hz, 6H), 5.39 (dt, $J = 15.4$, 7.3 Hz, 1H), 4.52 (d, $J = 3.1$ Hz, 1H), 4.13 (dd, $J = 13.3$, 7.3 Hz, 1H), 3.97–3.91 (m, 2H), 3.78 (s, 9H), 3.55–3.47 (m, 1H), 3.22–3.15 (m, 1H), 2.14–1.96 (m, 4H). ^{13}C NMR (151 MHz, MeOD) δ 173.3, 159.8, 150.6, 138.7, 132.1, 120.8, 114.2, 69.0, 68.1, 60.2, 56.9, 56.0, 55.7, 25.0, 23.3.

Synthesis of (*R*)-2-hydroxy-2-((*S*)-1-((E)-4,4,4-tris(4-methoxyphenyl)but-2-en-1-yl)pyrrolidin-2-yl)acetic acid (2*R*,2´*S*)-7g Obtained from (2*R*,2´*S*)-**39g** (38 mg, 0.07 mmol) according to Method G as a white solid in 45% yield. R_t (LC-MS) = 4.473 min. LC-MS (ESI): *m/z* calcd. for $C_{31}H_{36}NO_6^+$ $[M + H]^+ = 518.25$, found 518.3. R_t (HPLC) = 13.68 min. ^{1}H NMR (600 MHz, MeOD) δ 7.05 (d, $J = 15.4$ Hz, 1H), 6.97 (d, $J = 8.9$ Hz, 6H), 6.84 (d, $J = 8.9$ Hz, 6H), 5.38 (ddd, $J = 15.4$, 8.3, 6.3 Hz, 1H), 4.27 (d, $J = 6.2$ Hz, 1H), 4.13 (dd, $J = 13.2$, 6.3 Hz, 1H), 3.88–3.80 (m, 2H), 3.78 (s, 9H), 3.49–3.41 (m, 1H), 3.23–3.16 (m, 1H), 2.35–2.26 (m, 1H), 2.12–1.97 (m, 3H). ^{13}C NMR (151 MHz, MeOD) δ 174.4, 160.0, 150.8, 139.0, 132.4, 121.2, 114.5, 71.2, 69.8, 60.6, 59.1, 56.0, 55.4, 29.1, 23.9.

Synthesis of (*R*)-2-hydroxy-2-((*R*)-1-((E)-4,4,4-tris(4-methoxyphenyl)but-2-en-1-yl)pyrrolidin-2-yl)acetic acid (2*R*,2´*R*)-7g Obtained from (2*R*,2´*R*)-**39g** (19 mg, 0.04 mmol) according to Method G as a white solid in 32% yield. HPLC, LC-MS, ^{1}H NMR and ^{13}C NMR data as for (2*S*,2´*S*)-**7g**.

Synthesis of (*S*)-2-hydroxy-2-((*R*)-1-((E)-4,4,4-tris(4-methoxyphenyl)but-2-en-1-yl)pyrrolidin-2-yl)acetic acid (2*S*,2´*R*)-7g Obtained from (2*S*,2´*R*)-**39g** (35 mg, 0.07 mmol) according to Method G as a white solid in 66% yield. HPLC, LC-MS, ^{1}H NMR and ^{13}C NMR data as for (2*R*,2´*S*)-**7g**. HRMS (MALDI) *m/z* calcd. for $C_{31}H_{36}NO_6$ $[M + H]^+ = 518.2543$, found: 518.2547.

Synthesis of (E)-4,4',4''-(4-bromobut-2-ene-1,1,1-triyl)tris(-methoxybenzene) 40 4,4',4''-(chloromethanetriyl)tris(-methoxybenzene) (5.00 g, 13.36 mmol) was dissolved in acetonitrile (125 ml) and stirred vigorously. A solution of NaOH (1 M, 20 ml, 1.5 eq) was added dropwise and the reaction mixture was stirred at 40 °C overnight. Upon dilution with water (30 ml), the acetonitrile was evaporated under vacuum, and the aqueous solution was extracted with diethyl ether (5 × 15 ml). The combined organic phase was dried over anhydrous sodium sulfate, filtered, and the solvent was removed under vacuum, providing tris(4-methoxyphenyl)methanol as a viscous orange oil in 98% yield, that was used without further purification. ^{1}H NMR (400 MHz, $CDCl_3$) δ 7.17 (d, $J = 8.8$ Hz, 6H), 6.83 (d, $J = 8.8$ Hz, 6H), 3.80 (s, 9H), 2.65 (bs, 1H). ^{13}C NMR (101 MHz, $CDCl_3$) δ 158.8, 139.9, 129.2, 113.3, 81.3, 55.4. The crude (4.65 g, 12.61 mmol) and allyltributyltin

(8.13 ml, 8.77 g, 26.48 mmol, 2.1 eq) were dissolved in DCM (40 ml), and BF_3-OEt_2 (3,27 ml, 3.76 g, 26.48 mmol, 2.1 eq) was added dropwise. The reaction mixture was stirred at room temperature for 6 h. Upon quenching by addition of a saturated solution of $NaHCO_3$, the aqueous layer was extracted three times with DCM. The combined organic layers were dried over anhydrous sodium sulfate, filtered and the solvent was evaporated under reduced pressure, providing a crude that was purified by flash column chromatography (heptane/EtOAc 7:3 + 5% TEA). 4,4',4''-(but-3-ene-1,1,1-triyl)tris(methoxybenzene) was obtained as a white solid in 83% yield. ^{1}H NMR (600 MHz, $CDCl_3$) δ 7.09 (d, $J = 8.9$ Hz, 6H), 6.79 (d, $J = 8.9$ Hz, 6H), 5.67 (ddt, $J = 17.2$, 10.3, 6.6 Hz, 1H), 5.02 (dq, $J = 17.2$, 1.5 Hz, 1H), 4.94 (dq, $J = 10.3$, 1.5 Hz, 1H), 3.78 (s, 9H), 3.34 (dt, $J = 6.6$, 1.5 Hz, 2H). ^{13}C NMR (151 MHz, $CDCl_3$) δ 157.6, 140.2, 136.5, 130.4, 117.2, 113.1, 55.3, 54.4, 46.2. The intermediate 4,4',4''-(but-3-ene-1,1,1-triyl)tris(methoxybenzene) (3.00 g, 8.01 mmol, 1 eq) was dissolved in CCl_4 (30 ml), and NBS (1.43 g, 8.01 mmol, 1 eq) and AIBN (79 mg, 0.48 mmol, 0.06 eq) were added. The reaction mixture was refluxed overnight and controlled by NMR. The suspension was filtered, and the filtrate was evaporated under vacuum. The residue was purified by flash column chromatography (gradient from heptane to heptane/EtOAc 9/1) providing the desired product **40** as a viscous pale yellow oil in 66% yield. ^{1}H NMR (400 MHz, $CDCl_3$) δ 6.96 (d, $J = 8.9$ Hz, 6H), 6.81 (d, $J = 8.9$ Hz, 7H), 6.72 (dd, $J = 15.3$, 1.0 Hz, 1H), 5.52 (dt, $J = 15.3$, 7.7 Hz, 1H), 4.09 (dd, $J = 7.7$, 1.0 Hz, 2H), 3.80 (s, 9H). ^{1}H-NMR data in accordance to literature [30].

Pharmacology

Materials

Dulbecco's Phosphate Buffered Saline (DPBS), Dulbecco's modified Eagle medium (DMEM) with GlutaMAX-I, Ham's F12 Nutrient Mix, Hanks Balanced Salt Solution (HBSS), fetal bovine serum (FBS), penicillin-streptomycin (P/S), hygromycin B and tryspin-EDTA were purchased from Life Technologies (Paisley, UK). Poly-D-lysine (PDL), GABA, $CaCl_2$, $MgCl_2$ and HEPES (4-(2-hydroxyethyl)piperazine-1ethanesulfonic acid) were purchased from Sigma-Aldrich (St. Louis, MO, USA). FLIPR Membrane Potential (FMP) Blue Dye was purchased from Molecular Devices (Crawley, UK). PolyFect transfection reagent was obtained from Qiagen (West Sussex, United Kingdom). Plasmocin was purchased from InvivoGen (San Diego, CA, USA). [2,3-^{3}H(N)]GABA (specific activity 35 Ci/mmol) and MicroScint™20 were purchased from PerkinElmer (Boston, MA, United States). [2,2-^{3}H(N)] taurine (specific activity 19 Ci/mmol) was a kind gift from Prof. Harald Sitte, University of Vienna, Austria.

Cell culturing and transfection

The tsA201 cell line as well as the Flp-In CHO cell lines stably expressing hGATs were engineered and maintained as previously described [24, 39, 51]. Briefly, tsA201 cells were cultured in DMEM supplemented with 10% FBS and 1% P/S, whereas Flp-In hGAT CHO cells were cultured in Ham's F12 Nutrient Mix supplemented with 10% FBS, 1% P/S and plasmocin (5 µg/ml) under the selection pressure of hygromycin B (200 µg/ml). TsA201 cells were transfected with 8 µg of plasmids of previously described origin ((hGAT-pcDNA5/FRT) [39] or hTauT (pUNIV) [52]) per 10 cm dish using Polyfect transfection reagent according to the manufacturer's protocol (Qiagen), but with half of the recommended PolyFect volume.

[^{3}H]GABA and [^{3}H]taurine uptake assay

The [^{3}H]GABA and [^{3}H]taurine uptake assays were performed as previously described [17, 24, 39]. Briefly, assay buffer contained HBBS supplemented with 20 mM HEPES, 1 mM $CaCl_2$ and 1 mM $MgCl_2$. White 96-well polystyrene cell culture plates (PerkinElmer, USA) were coated with PDL and cells plated at a density of 50,000 cells/well a day before the assay. For radioligand-based uptake assays cells were incubated with 30 nM of [^{3}H]GABA or 22 nM of [^{3}H]taurine with or without dilutions of compounds for 3 or 5 min at 37 °C, respectively. Followed by washing and draining of liquid from the wells, 150 µl Microscint-20 was added per well, and after shaking, plates were counted in a TopCount NXT Microplate Scintillation & Luminescence Counter (PerkinElmer). Full uptake was determined with radioligand alone and full inhibition in the presence of either 3 mM GABA for the GATs and 3 mM taurine for the TauT.

The FLIPR membrane potential (FMP) assay

The FMP assay was performed to functually characterize the electrogenic transport of (2*S*,2´*S*)-**6** and (2*S*,2´*S*)-**7** via hGAT3 and hGAT1 transiently expressed in tsA201 cells. The assay was performed as previsouly described [53]. Briefly, cells were plated (50,000/well) into black PDL-coated 96-well plates with clear bottoms (VWR, Radnor, PA, USA). On the next day, cells were washed with HBSS assay buffer, FMP Blue Dye was added and the plate was incubated for 30 min at 37 °C. The cell plate was then assayed in a FlexStation 3 Benchtop Multi-Mode Microplate Reader (Molecular Devices). The ligand plate was placed into the FlexStation 15 min before reading of the cell

plate to ensure preheating to 37 °C. The fluorescence signals were measured 33.8 s after ligand addition at an emission and excitation wavelength of 560 nm and 530 nm, respectively. The signal was measured as the change in fluorescence units (ΔFU) between peak fluorescence before and after compound addition.

Data analysis

Data analysis was performed with Graphad Prism 9.5. Data Visualization of the screening data for Figs. 3A and 6 where performed in RStudio 2022.12.0 with R 4.1.2 and the package ggplot2 3.3.6. The screening data of compounds **1**–**12** were normalized to 100% [^{3}H]GABA uptake and presented as the mean of remaining [^{3}H]GABA residual activity of either a single or two independent experiments with three technical replicates. Concentration-response curves from radioligand uptake experiments were fitted by non-linear regression to a sigmoidal curve with variable slop according to the following equation: $Y = \text{Bottom} + (\text{Top–Bottom})/(1 + 10\text{^}((\log\text{IC50} - X) \times \text{HillSlope}))$, where Y is the response, Top and Bottom are the plateaus in the same units as Y, X is the logarithm of the concentration, logIC50 is the concentration where the response is halfway between the top and the bottom plateus, and HillSlope describes the steepness of the curve.

[^{3}H]Muscimol binding assay in rat synaptic membranes

The [^{3}H]muscimol binding assays was performed at rat cortical synaptic membranes in a 96-well microplate as previously described [54]. Briefly, compounds were incubated with [^{3}H]muscimol and membranes at 0–4 °C, filtered through GF/C filter plates (PerkinElmer) using a 96-well harvester (Packard), rapidly washed three times with ice-cold binding buffer, and the filter plates were dried. The CPM values were determined using liquid scintillation counting in a TopCount NXT Microplate Scintillation & Luminescence Counter (PerkinElmer). The CPM values were fitted by non-linear regression using GraphPad Prism 7.0 (GraphPad Software, San Diego, CA), and the IC50 values were determined and converted to Ki values using the Cheng–Prusoff equation. The experiments were performed in triplicate at least three times for each compound. Nonspecific binding was determined using 1.0 mM GABA.

Molecular modeling

Conformational searches were carried out either in water (for (*S*)-isoserine, (2*S*,2´*S*)-**6** and (2*S*,2´*S*)-**7**) or in chloroform (for (2*S*,2´*S*)-**21** and (2*R*,2´*S*)-**21**), using the Monte Carlo Minimum Method (MCMM) with Polak-Ribiere Conjugate Gradient (PRCG) minimization included in the Macromodel module of Schrödinger, with default settings (force field: OPLS4).

Supplementary information The online version contains supplementary material available at https://doi.org/10.1007/s00044-023-03126-7.

Acknowledgements This work was supported by the Lundbeck Foundation grants R303-2018-3346 and R347-2020-2381, the Novo Nordisk Foundation grants NNF21OC0067835 and NFF20OC0065017 and Simon Fougner Hartmanns Familiefond.

Author contributions FB designed the study, synthesized most of the compounds, wrote the first draft and revised the manuscript with help from all co-authors. MEKL, SK and KSW performed the biological assays. CA synthesized compounds. PW and BF supervised the work and critically reviewed the manuscript. All authors approved the final manuscript.

Funding Open access funding provided by Royal Library, Copenhagen University Library.

Compliance with ethical standards

Conflict of interest The authors declare no competing interests.

References

1. Lee V, Maguire J. The impact of tonic GABAA receptor-mediated inhibition on neuronal excitability varies across brain region and cell type. Front Neural Circuits. 2014;8. https://doi.org/10.3389/fncir.2014.00003.
2. Fattorini G, Melone M, Conti F. A reappraisal of GAT-1 localization in neocortex. Front Cell Neurosci. 2020;14. https://doi.org/10.3389/fncel.2020.00009.
3. Łątka K, Jończyk J, Bajda M. γ-Aminobutyric acid transporters as relevant biological target: their function, structure, inhibitors and role in the therapy of different diseases. Int J Biol Macromol. 2020;158:750–72. https://doi.org/10.1016/j.ijbiomac.2020.04.126.
4. Scimemi A. Structure, function, and plasticity of GABA transporters. Front Cell Neurosci. 2014;8. https://doi.org/10.3389/fncel.2014.00161.

5. Xu M-Y, Wong AHC. GABAergic inhibitory neurons as therapeutic targets for cognitive impairment in schizophrenia. Acta Pharmacol Sin. 2018;39:733–53. https://doi.org/10.1038/aps.2017.172.
6. Righes Marafiga J, Vendramin Pasquetti M, Calcagnotto ME. GABAergic interneurons in epilepsy: more than a simple change in inhibition. Epilepsy Behav. 2021;121:106935. https://doi.org/10.1016/j.yebeh.2020.106935.
7. Goodspeed K, Pérez-Palma E, Iqbal S, Cooper D, Scimemi A, Johannesen KM, et al. Current knowledge of SLC6A1-related neurodevelopmental disorders. Brain Commun. 2020;2. https://doi.org/10.1093/braincomms/fcaa170.
8. Lie MEK, Al-Khawaja A, Damgaard M, Haugaard AS, Schousboe A, Clarkson AN, et al. Glial GABA transporters as modulators of inhibitory signalling in epilepsy and stroke. Adv Neurobiol. 2017;16:137–67.
9. Damgaard M, Haugaard AS, Kickinger S, Al-Khawaja A, Lie MEK, Ecker GF, et al. Development of non-GAT1-selective inhibitors: challenges and achievements. Adv Neurobiol. 2017;16:315–32.
10. Schachter SC. Pharmacology and clinical experience with tiagabine. Expert Opin Pharmacother. 2001;2:179–87. https://doi.org/10.1517/14656566.2.1.179.
11. Treiman DM. GABAergic mechanisms in epilepsy. Epilepsia. 2001;42:8–12. https://doi.org/10.1046/j.1528-1157.2001.042suppl.3008.x.
12. Chiu CS. GABA transporter deficiency causes tremor, ataxia, nervousness, and increased GABA-induced tonic conductance in cerebellum. J Neurosci. 2005;25:3234–45. https://doi.org/10.1523/jneurosci.3364-04.2005.
13. Schousboe A, Madsen KK, White HS. GABA transport inhibitors and seizure protection: the past and future. Future Med Chem. 2011;3:183–7. https://doi.org/10.4155/fmc.10.288.
14. Andersen JV, Jakobsen E, Westi EW, Lie MEK, Voss CM, Aldana BI, et al. Extensive astrocyte metabolism of gamma-aminobutyric acid (GABA) sustains glutamine synthesis in the mammalian cerebral cortex. Glia. 2020;68:2601–12. https://doi.org/10.1002/glia.23872.
15. Clarkson AN, Huang BS, Macisaac SE, Mody I, Carmichael ST. Reducing excessive GABA-mediated tonic inhibition promotes functional recovery after stroke. Nature. 2010;468:305–9. https://doi.org/10.1038/nature09511.
16. Crunelli V, Lőrincz ML, McCafferty C, Lambert RC, Leresche N, Di Giovanni G, et al. Clinical and experimental insight into pathophysiology, comorbidity and therapy of absence seizures. Brain. 2020;143:2341–68. https://doi.org/10.1093/brain/awaa072.
17. Lie ME, Gowing EK, Johansen NB, Dalby NO, Thiesen L, Wellendorph P, et al. GAT3 selective substrate l-isoserine upregulates GAT3 expression and increases functional recovery after a focal ischemic stroke in mice. J Cereb Blood Flow Metab. 2019;39:74–88. https://doi.org/10.1177/0271678x17744123.
18. Andreß JC, Böck MC, Höfner G, Wanner KT. Synthesis and biological evaluation of α- and β-hydroxy substituted amino acid derivatives as potential mGAT1–4 inhibitors. Med Chem Res. 2020;29:1321–40. https://doi.org/10.1007/s00044-020-02548-x.
19. Wipf P, Skoda EM, Mann A. Chapter 11—Conformational restriction and steric hindrance in medicinal chemistry. In: Wermuth CG, Aldous D, Raboisson P, Rognan D, editors. The practice of medicinal chemistry. 4th ed. San Diego: Academic Press; 2015. p. 279–99.
20. Bavo F, Pallavicini M, Pucci S, Appiani R, Giraudo A, Eaton B, et al. From 2-triethylammonium ethyl ether of 4-stilbenol (MG624) to selective small-molecule antagonists of human α9α10 nicotinic receptor by modifications at the ammonium ethyl residue. J Med Chem. 2022;65:10079–97. https://doi.org/10.1021/acs.jmedchem.2c00746.
21. Krall J, Bavo F, Falk-Petersen CB, Jensen CH, Nielsen JO, Tian Y, et al. Discovery of 2-(imidazo[1,2-b]pyridazin-2-yl)acetic acid as a new class of ligands selective for the γ-hydroxybutyric acid (GHB) high-affinity binding sites. J Med Chem. 2019;62:2798–813. https://doi.org/10.1021/acs.jmedchem.9b00131.
22. Krall J, Jensen CH, Bavo F, Falk-Petersen CB, Haugaard AS, Vogensen SB, et al. Molecular hybridization of potent and selective γ-hydroxybutyric acid (GHB) ligands: design, synthesis, binding studies, and molecular modeling of novel 3-hydroxycyclopent-1-enecarboxylic acid (HOCPCA) and trans-γ-hydroxycrotonic acid (T-HCA) analogs. J Med Chem. 2017;60:9022–39. https://doi.org/10.1021/acs.jmedchem.7b01351.
23. Kobayashi T, Suemasa A, Igawa A, Ide S, Fukuda H, Abe H, et al. Conformationally restricted GABA with bicyclo[3.1.0]hexane backbone as the first highly selective BGT-1 inhibitor. ACS Med Chem Lett. 2014;5:889–93. https://doi.org/10.1021/ml500134k.
24. Al-Khawaja A, Petersen JG, Damgaard M, Jensen MH, Vogensen SB, Lie MEK, et al. Pharmacological identification of a guanidine-containing β-alanine analogue with low micromolar potency and selectivity for the betaine/GABA transporter 1 (BGT1). Neurochem Res. 2014;39:1988–96. https://doi.org/10.1007/s11064-014-1336-9.
25. Giraudo A, Krall J, Bavo F, Nielsen B, Kongstad KT, Rolando B, et al. Five-membered *N*-heterocyclic scaffolds as novel amino bioisosteres at γ-aminobutyric acid (GABA) type A receptors and GABA transporters. J Med Chem. 2019;62:5797–809. https://doi.org/10.1021/acs.jmedchem.9b00026.
26. Wein T, Petrera M, Allmendinger L, Höfner G, Pabel J, Wanner KT. Different binding modes of small and large binders of GAT1. ChemMedChem. 2016;11:509–18. https://doi.org/10.1002/cmdc.201500534.
27. Kickinger S, Al-Khawaja A, Haugaard AS, Lie MEK, Bavo F, Löffler R, et al. Exploring the molecular determinants for subtype-selectivity of 2-amino-1,4,5,6-tetrahydropyrimidine-5-carboxylic acid analogs as betaine/GABA transporter 1 (BGT1) substrate-inhibitors. Sci Rep. 2020;10. https://doi.org/10.1038/s41598-020-69908-w.
28. Watanabe M, Hirokawa T, Kobayashi T, Yoshida A, Ito Y, Yamada S, et al. Investigation of the bioactive conformation of histamine H_3 receptor antagonists by the cyclopropylic strain-based conformational restriction strategy. J Med Chem. 2010;53:3585–93. https://doi.org/10.1021/jm901848b.
29. Steffan T, Renukappa-Gutke T, Höfner G, Wanner KT. Design, synthesis and SAR studies of GABA uptake inhibitors derived from 2-substituted pyrrolidine-2-yl-acetic acids. Bioorg Med Chem. 2015;23:1284–306. https://doi.org/10.1016/j.bmc.2015.01.035.
30. Pabel J, Faust M, Prehn C, Wörlein B, Allmendinger L, Höfner G, et al. Development of an (*S*)-1-{2-[tris(4-methoxyphenyl)methoxy]ethyl}piperidine-3-carboxylic acid [(*S*)-SNAP-5114] carba analogue inhibitor for murine γ-aminobutyric acid transporter type 4. ChemMedChem. 2012;7:1245–55. https://doi.org/10.1002/cmdc.201200126.
31. Jacobsen P, Schaumburg K, Larsen J-J, Krogsgaard-Larsen P. Syntheses of some amino piperidine carboxylic acids related to nipecotic acid. Acta Chem Scand B.1981;35:289–94.
32. De Luca L, Giacomelli G, Porcheddu A. A very mild and chemoselective oxidation of alcohols to carbonyl compounds. Org Lett. 2001;3:3041–3. https://doi.org/10.1021/ol016501m.
33. Hoye TR, Jeffrey CS, Shao F. Mosher ester analysis for the determination of absolute configuration of stereogenic (chiral) carbinol carbons. Nat Protoc. 2007;2:2451–8. https://doi.org/10.1038/nprot.2007.354.
34. Bolchi C, Bavo F, Gotti C, Fumagalli L, Fasoli F, Binda M, et al. From pyrrolidinyl-benzodioxane to pyrrolidinyl-pyridodioxanes, or from unselective antagonism to selective partial agonism at

α4β2 nicotinic acetylcholine receptor. Eur J Med Chem. 2017;125:1132–44. https://doi.org/10.1016/j.ejmech.2016.10.048.
35. Pallavicini M, Moroni B, Bolchi C, Cilia A, Clementi F, Fumagalli L, et al. Synthesis and α4β2 nicotinic affinity of unichiral 5-(2-pyrrolidinyl)oxazolidinones and 2-(2-pyrrolidinyl)benzodioxanes. Bioorg Med Chem Lett. 2006;16:5610–5. https://doi.org/10.1016/j.bmcl.2006.08.020.
36. Bavo F, Pallavicini M, Gotti C, Appiani R, Moretti M, Colombo SF, et al. Modifications at C(5) of 2-(2-pyrrolidinyl)-substituted 1,4-benzodioxane elicit potent α4β2 nicotinic acetylcholine receptor partial agonism with high selectivity over the α3β4 subtype. J Med Chem. 2020;63:15668–92. https://doi.org/10.1021/acs.jmedchem.0c01150.
37. Hiraga Y, Widianti T, Kunishi T, Abe M. The cooperative effect of a hydroxyl and carboxyl group on the catalytic ability of novel β-homoproline derivatives on direct asymmetric aldol reactions. Tetrahedron: Asymmetry. 2011;22:226–37. https://doi.org/10.1016/j.tetasy.2011.01.025.
38. Sitka I, Allmendinger L, Fülep G, Höfner G, Wanner KT. Synthesis of *N*-substituted acyclic β-amino acids and their investigation as GABA uptake inhibitors. Eur J Med Chem. 2013;65:487–99. https://doi.org/10.1016/j.ejmech.2013.04.063.
39. Kvist T, Christiansen B, Jensen AA, Brauner-Osborne H. The four human γ-aminobutyric acid (GABA) transporters: pharmacological characterization and validation of a highly efficient screening assay. Comb Chem High Throughput Screen. 2009;12:241–9. https://doi.org/10.2174/138620709787581684.
40. Kragler A, Höfner G, Wanner KT. Novel parent structures for inhibitors of the murine GABA transporters mGAT3 and mGAT4. Eur J Pharmacol. 2005;519:43–7. https://doi.org/10.1016/j.ejphar.2005.06.053.
41. Kickinger S, Hellsberg E, Frølund B, Schousboe A, Ecker GF, Wellendorph P. Structural and molecular aspects of betaine-GABA transporter 1 (BGT1) and its relation to brain function. Neuropharmacology. 2019;161:107644. https://doi.org/10.1016/j.neuropharm.2019.05.021.
42. Schrödinger Release 2022-1: MacroModel. New York, NY: Schrödinger, LLC; 2021.
43. Wu Z, Guo Z, Gearing M, Chen G. Tonic inhibition in dentate gyrus impairs long-term potentiation and memory in an Alzheimer's disease model. Nat Commun. 2014;5:4159. https://doi.org/10.1038/ncomms5159.
44. Song I, Volynski K, Brenner T, Ushkaryov Y, Walker M, Semyanov A. Different transporter systems regulate extracellular GABA from vesicular and non-vesicular sources. Front Cell Neurosci. 2013;7. https://doi.org/10.3389/fncel.2013.00023.
45. Geoghegan K, Bode JW. Bespoke SnAP reagents for the synthesis of C-substituted spirocyclic and bicyclic saturated N-heterocycles. Org Lett. 2015;17:1934–7. https://doi.org/10.1021/acs.orglett.5b00618.
46. Yamamoto S, Sugimoto H, Tamura O, Mori T, Matsuo N, Ishibashi H. Synthesis of 3,3,3-trifluoroprop-1-enyl compounds from some enolizable aldehydes. Tetrahedron. 2004;60:8919–27. https://doi.org/10.1016/j.tet.2004.07.030.
47. Fjelbye K, Marigo M, Clausen RP, Juhl K. Enantioselective fluorination of spirocyclic β-prolinals using enamine catalysis. Synlett. 2017;28:425–8. https://doi.org/10.1055/s-0036-1588100.
48. Zhang D, Li P, Gao Y, Song Y, Zhu Y, Su H, et al. Discovery of a candidate containing an (S)-3,3-difluoro-1-(4-methylpiperazin-1-yl)-2,3-dihydro-1H-inden scaffold as a highly potent pan-inhibitor of the BCR-ABL kinase including the T315I-resistant mutant for the treatment of chronic myeloid leukemia. J Med Chem. 2021;64:7434–52. https://doi.org/10.1021/acs.jmedchem.1c00082.
49. Stephens BE, Liu F. A regio- and diastereoselective intramolecular nitrone cycloaddition for practical 3- and 2,3-disubstituted piperidine synthesis from γ-butyrolactone. J Org Chem. 2009;74:254–63. https://doi.org/10.1021/jo8018285.
50. Delany PK, Hodgson DM. Synthesis and homologation of an azetidin-2-yl boronic ester with α-lithioalkyl triisopropylbenzoates. Org Lett. 2019;21:9981–4. https://doi.org/10.1021/acs.orglett.9b03901.
51. Kragholm B, Kvist T, Madsen KK, Jorgensen L, Vogensen SB, Schousboe A, et al. Discovery of a subtype selective inhibitor of the human betaine/GABA transporter 1 (BGT-1) with a non-competitive pharmacological profile. Biochem Pharmacol. 2013;86:521–8. https://doi.org/10.1016/j.bcp.2013.06.007.
52. Al-Khawaja A, Haugaard AS, Marek A, Löffler R, Thiesen L, Santiveri M, et al. Pharmacological characterization of [^{3}H]ATPCA as a substrate for studying the functional role of the betaine/GABA transporter 1 and the creatine transporter. ACS Chem Neurosci. 2018;9:545–54. https://doi.org/10.1021/acschemneuro.7b00351.
53. Kickinger S, Lie MEK, Suemasa A, Al-Khawaja A, Fujiwara K, Watanabe M, et al. Molecular determinants and pharmacological analysis for a class of competitive non-transported bicyclic inhibitors of the betaine/GABA transporter BGT1. Front Chem. 2021;9. https://doi.org/10.3389/fchem.2021.736457.
54. Bavo F, de-Jong H, Petersen J, Falk-Petersen CB, Löffler R, Sparrow E, et al. Structure–activity studies of 3,9-diazaspiro[5.5]undecane-based γ-aminobutyric acid type A receptor antagonists with immunomodulatory effect. J Med Chem. 2021;64:17795–812. https://doi.org/10.1021/acs.jmedchem.1c00290.